CHALMERS

Bone Conduction Transducers and Output Variability

Lumped-parameter modelling of state variables

Master of Science Thesis in Biomedical Engineering

HERMAN LUNDGREN

Department of Signals and Systems
Biomedical Signals and Systems Division
CHALMERS UNIVERSITY OF TECHNOLOGY
Göteborg, Sweden, 2010
Report No. EX0042/2010

Title: Bone Conduction Transducers and Output Variability

Subtitle: Lumped-parameter modelling of state variables

Report No. EX042/2010

Chalmers Institute of Technology

Göteborg, Sweden, 2010

Department of Signals and Systems
Biomedical Signals and Systems

Abstract

Bone-conduction transducers for hearing aids are used by thousands of patients that cannot use conventional air-conduction hearing devices. Such bone conduction transducers have also been extensively used in bone conduction audiometry, for example, hearing threshold measurements. The interaction between these transducers output impedance and the patients skin impedance over the temporal bone, which both are in the same range, results in a high variability of the output force, acceleration and power which is directly related to the variability in the patients skin impedances. Because the output force is used as the reference zero standard for bone conduction hearing thresholds, variability in patient skin impedances is a source of error in threshold determination via bone conduction. This work investigates the extent of this variability in the output from one Radioear B71 transducer due to the skin impedances of 30 subjects. In the frequency range 100-10000 Hz, an inter subject standard deviation in the skin impedance, averaging 2.4 dB, gives rise to a standard deviation in force and acceleration output ranging from 0 - 5 dB. The impedance characteristic of the transducer can be used to predict which frequency regions correspond to increased output variability, as well as to find "golden" frequency areas having less force and acceleration output variability.

Contents

1 Introduction

Hearing impairment and deafness affect a significant portion of the world's population today. Precise demographics are difficult to obtain - due in part to the unwillingness of many to consider themselves as "disabled" - but existing statistics suggest that a significant portion of the world's population is affected. The Swedish agency HRF (Hörelseskadades Riksförbund) reported statistics in 2009 from CSB (Centrala Statistikbyrån) showing that 17.2% of Swedish people had qualified themselves as hard of hearing or hearing impaired (hereafter referred to as *hearing impaired* or as having *impaired hearing* or *hearing loss*) by CSB's standard. Of these nearly 1.3 million people, approximately 30% use an assistive device such as a hearing aid, and an estimated 60% could gain benefit from the use of one (HRF, 2009). Impaired hearing can come as a result of congenital defects or damage to the hearing organs due to disease or trauma and can for many significantly affect the quality of life. These statistics show a clear need for hearing aids, and there are numerous different devices and manufacturers available on the market to assist in improving hearing for those who can and wish to use them. A relatively small portion of those with impaired hearing are unable to use the traditional air-conducting (AC) hearing devices, but can gain benefit from the use of a bone-conducting device such as are studied in this work. Bone-conducting (BC) devices are being increasingly used to assist those with suitable needs, and the need for improvement and development of these products is growing as well.

When attempting to determine the type and level of hearing loss in a patient, a hearing test is performed, normally measuring hearing thresholds. Hearing thresholds are then used to evaluate a suitable treatment, whether it be surgery, drugs, taking no action at all or the use of a hearing aid. The standards for hearing thresholds is called *audiometric zero* and is based on measurements taken from average normal-hearing young adults. For AC devices the standards are measured in sound pressure. For BC transducers, the standards for audiometric zero (ISO, 1994) are given in force, and have been defined by the use of RETFLs (Reference Equivalent Threshold Force Levels) and a device called an artificial mastoid which simulates the acoustic properties of the mastoid portion of the skull bone. The force experienced at the mastoid portion of the skull (where the BC device is normally applied) is dependent on the mechanical impedance (complex mechanical resistance) of the subject's skull, by the relationship

$$Z(j\omega) = \frac{F(j\omega)}{v(j\omega)} \tag{1}$$

where $Z(j\omega)$ (the skin impedance) is the mechanical point impedance of the skull seen from outside the skin at the mastoid, $v(j\omega)$ is the vibrational

velocity and $F(j\omega)$ is the force produced at the mastoid at a given angular frequency ω. The variation in individual Z has been shown to be considerable (Cortes, 2002) and may result in variability in force and velocity produced at the transducer/skin interface by the BC transducer. A study of the behaviour of this system is helpful in understanding the significance and accuracy of the existing standards in audiometry.

2 Background/Theory

2.1 Biology and Mechanics of Hearing

Human beings and many other organisms on earth use auditory sensing - known in their case as hearing - to perceive their surroundings. The ear (See figure 1) is the primary sensing organ for sound and consists of three parts. The outer ear filters, reflects, amplifies, and transmits sound to the middle ear. It consists of the external cartilage and skin (known as the *pinna*) and the auditory canal, a soft tube which leads to the *tympanic membrane*, or ear drum. The middle ear is the air-filled cavity between the eardrum and the cochlea, and contains the three bones known as *ossicles*. These act as mechanical levers driven by the vibration of the tympanic membrane, and amplify the pressure of the vibrations as they are transmitted to the oval window, the beginning of the middle ear. The oval window is a membrane which separates the middle ear from cochlea, which contains the sensory organ of the inner ear. The cochlea is fluid-filled, and the vibrations propagated in this fluid stimulate the hair cells of the *organ of corti*, converting the mechanical vibrations to electrical action potentials in the hair cells for transmission via the auditory nerve to the brain for interpretation. In this sense the organ of corti acts as a transducer, and in humans it has the ability to receive and transduce sound signals with a dynamic range of $20 - 20k\ Hz$. The complexity of this organ is considerable, and for the scope of this work it will suffice to say that hearing sensitivity varies significantly over this frequency range.

The conduction of sound through the outer and middle ear is primarily via air and the soft tissue from the pinnae to the tympanic membrane, then by the bones of the ossicular chain and the air surrounding them. This is however only one path of conduction between the surroundings and the cochlea. Sound can also travel through the bones of the skull, surpassing the outer and middle ear entirely. As can be seen in figure 1, the inner ear is quite deep inside the head, and is surrounded by bone. When the bone vibrates, the cochlea can be directly stimulated, which produces the same sensation of hearing that is achieved through air conduction.

This type of sound conduction can be observed when speaking while occluding the ear canals with the fingers. The percieved volume of one's own voice is not significantly affected, as it is transmitted through BC via the teeth, jaw, hard palate and skull to the cochlea, though the transmission of low frequencies over high ones is quite prevalent. Unlike the own voice, however, the majority of sound reaches the cochlea almost exclusively via air conduction, which means that problems with the outer or middle ear can result in impaired hearing.

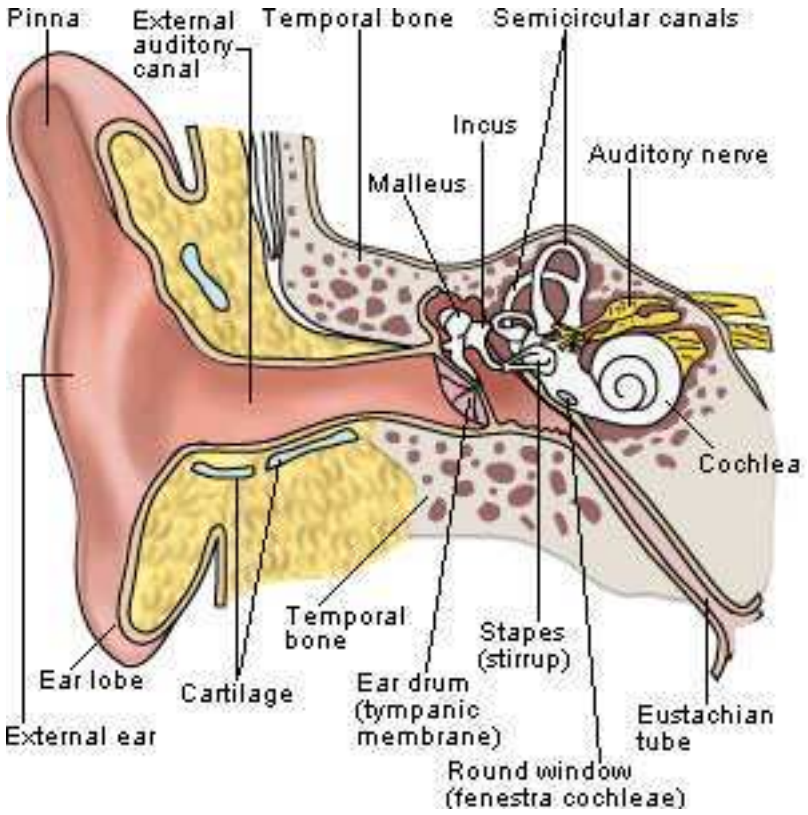

Figure 1: The anatomy of the ear. (*Image taken from: http://www.guadalupe-ec.org/*)

2.2 Hearing Loss

Hearing loss can be loosely grouped into: *sensorineural*, *conductive*, and *mixed*. Sensorineural hearing loss is due to impaired function of the inner ear, auditory nerve, or higher centra in the brain. If the sensitive hair cells in the organ of corti are damaged or defective, or if there is a problem with neural transmission or processing of the electrical signals produced therein, the impairment is considered sensorineural. This can in certain cases be treated by a cochlear implant, which is a device that directly stimulates nerve cells in the cochlea via electrodes, hence transducing the auditory signal from mechanical waves to electrical signals. Pure conductive hearing loss is characterised by a functioning sensorineural system, but with impaired acoustic/mechanical conduction of sound to the inner ear. This can depend on a number of factors such as occlusion of the hearing canal, damage or deformation of the middle ear, tumours, and obstruction of the oval window. Mixed hearing loss is any combination of conductive and sensorineural hearing loss.

The treatments for conductive hearing loss vary and can include surgery to physically alter the problematic region of the auditory pathway. A common method of treatment is the amplification of incoming sound to compensate for the problematic attenuation. This can be done by placing an AC loudspeaker device directly in the ear canal. These devices and their bulkier body-worn and table-top predecessors have been used since the early 20th century, before which a commonly used method was passive mechanical amplification of sound with an ear horn.

With some types of conductive and mixed hearing loss, the use of bone conduction to transfer sound to the cochlea is preferable to air conduction. These include patients for whom the obstruction/fixation of the ear canal is undesirable or impractical because of congenital malformation or chronic infection or eczema of the middle and outer ears, or those who have such impaired conduction in the middle ear that the gain obtained from air-conduction devices cannot compensate for the attenutation.

2.3 Audiology

When a patient is suspected of having a hearing impairment, they visit an audiologist to determine the severity and type of hearing loss they have. The audiologist performs an audiometric evaluation, which is normally a test of hearing thresholds at a number of different pure-tone frequencies within the range of human hearing. A complete pure-tone audiometry consists of testing hearing thresholds through air conduction and bone conduction.

Before the testing is done, the equipment is calibrated according to the ISO 389 series standard, and the patient is informed on how to indicate that they hear each test tone. They are placed in an anechoic sound insulated

test room where they have visual contact with the tester, and are fitted with insert or alternately supra- or circumaural headphones. The tester sends an audible pure tone at 1000 Hz to one of the headphones, then decreases the level of the tone in 10 dB steps until the patient no longer indicates that they can hear it. The level is then increased in 5 dB steps until the patient can hear the sound again. This procedure is repeated until the patient has responded on the same threshold level on two out of two, three, or four ascents (BSA, 2002). This is the threshold level of hearing for that frequency. The process is repeated with tones of frequencies $2000, 4000, 8000, 500$, and $250\ Hz$. If needed, the intermediate frequencies $750, 1500, 3000$, and $6000\ Hz$ can be tested as well. Retesting at $1\ kHz$ is done for the first ear, and if there is an acute difference of more than $5\ dB$ in threshold value, the other frequencies are retested as well. After this process is carried out for both ears, the bone conduction test is performed.

The procedures for bone conduction audiometric testing are similar or identical to the one for air conduction, with two important differences:

- the frequencies tested are usually limited to $500 - 4000\ Hz$ (BSA, 2002), and
- the need for masking becomes an important consideration.

The reduced range of frequencies depends on several factors. The standard BC hearing aid used for audiometery is the Radioear B71. As with other BC transducers, the B71 demonstrates high levels of total harmonic distortion (THD) at high signal levels and also at low frequencies (Stenfelt and Håkansson, 2002). Since THD is a measure of the ratio of total harmonic frequency power to fundamental frequency power, a high THD means significant overtone presence. This can lead to inaccurate measurements of the hearing threshold at frequencies with high THD, as the harmonic overtones could become audible at lower signal levels than the fundamental. An additional reason for not measuring BC thresholds at frequencies below $500\ Hz$ is the contribution of vibrotactile sensation. This refers to the ability to sense vibration rather than hear it, and the vibrotactile thresholds at low frequencies are such that vibrotactile sensation could give more acute hearing thresholds (as low as 25 dB hearing loss at $250\ Hz$)(Stenfelt and Håkansson, 2002). At higher frequencies, the performance of the B71 is also limited and the accuracy of the test becomes compromised. Above $2\ kHz$, the airborne sound radiation from the transducer housing can become sufficient to contribute to hearing sensation. This may result in inaccurately acute thresholds, and it is recommended by the British Society of Audiology that the ear canal of the ear being tested is occluded at frequencies of 3000 and $4000\ Hz$ (BSA, 2002).

With bone-conduction, there can be a significant amount of cross-hearing (between the two ears) due to transmission of the vibration through the skull bone to the contralateral cochlea. Whereas the transcranial attenuation sound with AC headphones can be significant (from $40-80$ dB BSA (2002)), bone conduction may cause as little as $0-20$ dB attenuation (BSA, 2004), and the sound can even be percieved as louder on the contralateral side than the ipsilateral (Håkansson et al., 2010). Since threshold differences between the ears can far exceed 20 dB, the sound may be detected by the opposing ear before the one being tested. When single-ear threshold testing is desired, this necessitates masking of the contralateral ear with narrow-band noise to elevate that ear's threshold. The procedures for masking will not be explained here, but can be found in the BSA guide referenced here (BSA, 2002). Standards for calibration levels can be found in ISO 389.

When AC and BC threshold tests have been done, the results are plotted in an audiogram, which shows the hearing threshold at each tested frequency in decibel hearing level (dBHL) relative to the standard audiometric zero specified in ISO 389. Audiometric zero represents the threshold of hearing for an average normal hearing person. The determination of audiometric zero for bone conduction uses a method involving an artificial mastoid, and is described below. There are several methods for determining where the hearing thresholds lie, but all should give a set of data showing the BC thresholds and one showing the AC thresholds. An example of an audiogram is seen in figure 2.3. By analysing the relation between these thresholds, the type of hearing loss can be roughly determined. A large and uniform gap between the AC and BC thresholds with BC thresholds being lower (more sensitive) indicates conductive hearing loss, while the coincidence of higher AC and BC thresholds can suggest that a hearing loss is sensorineural. Some diseases or conditions show a frequency-dependent hearing loss, and they can be diagnosed by the help of an audiogram as well.

2.3.1 Calibration for BC Audiometry

As mentioned above, before an audiometric test battery is conducted, it is essential that the equipment is calibrated so that audiometric zero (seen in figure 2.3 as the line marked 0 dB) represents the hearing thresholds of the average otologically normal hearing person. With AC, the calibration can be done by directly measuring the sound pressure at the output of the headphones and adjusting the signal strength accordingly. For BC devices, the force level at threshold cannot be measured directly without specialized equipment, and the standard measure of audiometric zero is a force produced by the BC device (normally a Radioear B71) on an artificial mastoid (AM) B&K type 4930, which is designed to indirectly measure the force output of the BC transducer. A correction is applied to this measured data to take into account that the force gauge is placed under the rubber pad of the B&K 4930.

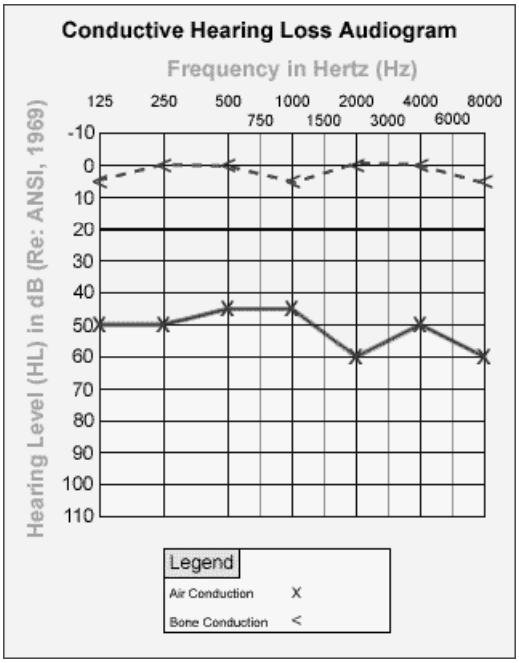

Figure 2: An example of an audiogram for BC and AC thresholds in one ear.(*Image taken from: http://www.osha.gov*)

This corrected force is known as the reference equivalent threshold force level (RETFL) and is defined as the force output on an AM when applying the same electrical input signal that produces a threshold-level sound when the BC device is attached to an average otologically normal person. Once the BC device is calibrated, the dB difference in signal strength between audiometric zero and the subject's threshold can be found and plotted in an audiogram. From equation 1, it can be seen that the force produced is dependent on the mechanical point impedance Z of the load. If the impedance of two loads such as an artificial mastoid and a human mastoid differs, the output force for a given input signal will differ as well, dependent on the electrical and mechanical properties of the BC device. It is known that the standard impedance for artificial mastoids differs from that of the average human mastoid. Consequently the force output may differ at the human mastoid and the artificial mastoid, and this is why the standard is referred to as a reference equivalent force level. This may be a cause of uncertainty in audiometric threshold determination, as the reference thresholds for audiometric zero and the measured thresholds are taken from different subjects. The error caused by these differences will be unknown at each audiometric test, but a knowledge of the potential error is still useful in the interpretation of results. The variability in force output due to variability in human mastoid

impedances, and the difference in force output on an AM and a human mastoid are therefore of interest.

2.3.2 Sources of Error

The accuracy of the audiometric measurements is important to enable proper analysis of hearing loss. Sources of error as well as intersubject and test-retest variability must be considered and accounted for. Conformance to standards ensures some accuracy, however, some sources of error and variability remain. These include:

- Position of device - small variations in placement on the mastoid can correspond to large variations in impedance.
- Contact pressure variability.
- Subject response error - many factors such as attentiveness, breathing and heartbeat sounds, and understanding of instructions may contribute.
- Operator error.
- Ambient noise contribution.
- Calibration error.

The importance of being able to account for threshold variability in audiometry increases when one considers the worst-case scenario, where the different errors and variabilities add up. An analysis of the total possible error and confidence intervals for determination of hearing thresholds by AC and BC requires a quantitative knowledge of the individual sources of error. As was adressed above, there are possible sources of variability and bias errors in the determination of BC thresholds that are known to exist, but are unknown in magnitude. A better quantitative knowledge of these factors is hence of importance to the field of audiology.

2.4 Bone Conduction Hearing Devices

BC devices, though far less common than AC devices have come to be in common use in the last few decades. For those who desire or require a BC device, there are two viable alternatives and one currently under development. The first and oldest type of BC device is the transcutaneous (through the intact skin). These devices consist of a transducer fixed in a casing which is pressed against the skull, normally behind the ear at the mastoid portion of the temporal bone. The device is held in place by a steel spring or a soft headband which provides the correct contact pressure. The second type is percutaneous (through the skin), and requires an implanted skin-penetrating

titanium screw. The screw is most commonly placed and anchored in the mastoid portion of the temporal bone about 55 mm behind the pinna, and after being osseointegrated is fitted with a post which protrudes from the skin to provide an attachment point for the transducer. The device is attached to the implant by a snap coupling to allow for easy release so as to minimize damage to the device and the implant upon accidental impact. The effectiveness of direct bone stimulation together with the added comfort and aesthetic appeal of a headband-free device have made the BAHA (*Bone Anchored Hearing Aid)* the preferable device for most. Equally as important is the increased quality of the conducted sound at lower power consumption made possible by the direct transmission of vibrations into the skull. The hearing device currently under development is the subcutaneous Bone-Conduction Implant (BCI), which will use an implantable transducer that is powered transcutaneously by electromagnetic induction. This type of device will provide the same benefits as BAHAs, but with the lack of a permanent opening in the skin for the titanium abutment.

2.4.1 The B71

The BC device used in most audiometry is the Radioear B71 (shown in figure 3). The device dimensions are $31 \times 18 \times 18$ mm, and it has a total weight of 22.3 g, not including the headband. It is held in place by a steel or soft fabric headband, which provides a contact pressure of approximately 5.4 N across a contact area of 2.0 cm^2. The exterior of the B71 consists of a plastic casing with two terminals on one short end for the input electrical signal. The round protruding portion of the casing is the contact surface which is pressed against the mastoid. The halves of the housing are held together by three screws, and the transducer inside is attached to the back of the casing with two screws. Figure 3(a) and 3(b) shows the casing and the transducer when removed from the casing.

The transducer is of variable-reluctance type, and consists of a magnetic armature suspended from the casing by the compliant side arms of a stiff metal plate (visible between the screws in figure 3(b)). The electrical signal passes through coils of wire which are wrapped around the armature, inducing a magnetic flux in the magnetic circuit consisting of the armature and the metal plate. The resultant force generated across the air gap in the circuit causes a deflection of the suspended plate, which manifests as harmonic vibrations when an alternating electrical signal is applied. This vibration is propagated through the plastic casing and into the skull of the user as sound.

2.5 Modelling and Simulation

For system-based engineering applications such as this one, analysis and quantification are needed at all stages of development. This analysis gener-

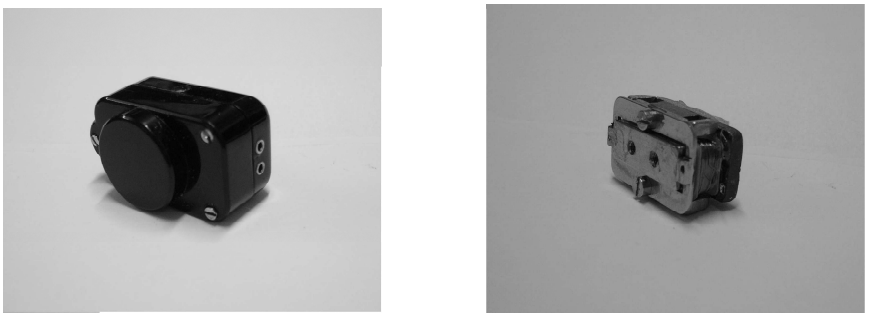

(a) (b)

Figure 3: (a) The B71 transducer with and (b) without its casing.

ally requires that system behaviour be quantified so that an objective comparison can be made between different decisions in the development process. The desired quantities to be extracted can be difficult or inefficient to measure directly (or impossible if the system does not yet exist) due to the need for equipment and subjects, time constraints, setup logistics, system complexity, and measurement and equipment error. An alternative to the direct measurement of parameters in a system is the use of a model for simulation. With the creation of an appropriate model a particular system can be simulated, providing the freedom to vary parameters of interest and observe the resulting changes in behaviour. An important benefit of simulation is the ability to simplify the system and isolate the outputs of interest. This and other benefits can far outweigh the drawbacks, provided that the model is well designed and consideration is taken of the potential contributions to system behaviour that are removed or simplified.

2.5.1 Electrical/Mechanical Analogies

The mathematical treatment of simple mechanical systems involves the use of linear differential equations to express the relationships between force, acceleration, velocity, and physical characteristics such as mass and compliance. Interestingly, these differential equations have exact analogies in the electrical domain and as a consequence, mechanical systems can be simplified and modelled as electrical systems and vice versa. These analogies are utilized in this work to model the electromechanical system of the B71 as a relatively simple electrical system.

There are two common analogues in the electrical domain, both of which start by defining potential and current as electrical analogues to mechanical quantities. In this work, force is represented by potential and velocity is represented by current. It will be demonstrated here how the analogue to mass is derived from these, then additional relevant analogues are presented in table 1.

Table 1: Mechanical-Electrical analogue quantities

Mechanical	Notation	Electrical	Notation
Force	F	Potential	u
Velocity	v	Current	i
Compliance	$c_m = \frac{1}{F}\int_{t1}^{t2} v(\tau)d\tau$	Capacitance	$C = \frac{1}{u}\int_{t1}^{t2} i(\tau)d\tau$
Mass	$m = \frac{F}{\frac{dv}{dt}}$	Inductance	$L = \frac{u}{\frac{di}{dt}}$
Damping	$R_m = \Re(\frac{F}{v})$	Resistance	$R = \Re(\frac{u}{i})$

Newton's second law can be written as:

$$F = m \cdot a = m \cdot \frac{dv}{dt} \tag{2}$$

Upon replacing the force F and the velocity v with their electrical equivalents, it becomes apparent that the mass m is equivalent to inductance L

$$u = L \cdot \frac{di}{dt} \tag{3}$$

The analogies for capacitance and resistance are derived similarly by using Hooke's and Ohm's laws respectively.

As in the electrical domain, the relationship between the force and the velocity at a given frequency is such that their quotient yields the *impedance* by equation 1, where Z denotes the complex impedance. Note that the calculation of resistance in table 1 is done by taking the real part of this quotient. When the force and velocity are taken at the same point, Z is referred to as driving-point impedance, which in this work will be referred to simply as impedance.

2.5.2 Two-Port Models

One way to model an electrical system is using a two-port network. An advantage of this model is that the parameters can be determined by direct measurement without any knowledge of the components of the system.

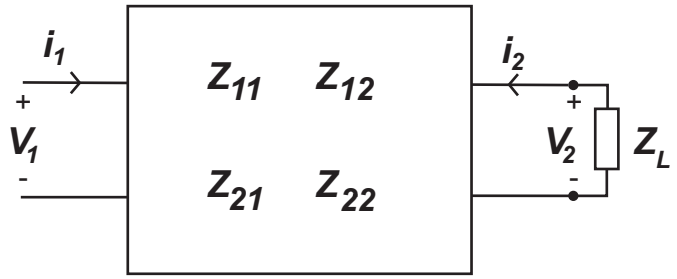

Figure 4: A "black box" two-port network with a load Z_L on the output side.

Provided that there are an output port and an input port (each with two terminals) satisfying the condition that the same current enters and leaves each port, the system can be considered a black box characterised only by four network parameters. The parameters themselves are determined by relationships between measured quantities at the ports, and can be impedances, admittances, or hybrids of the two. Figure 4 shows a two-port depiction of a linear electrical system using impedances as network parameters.

Since the B71 is a linear system composed of passive components, it can be and has in fact been modeled as a two-port network (Cortes, 2002). For the purposes of this work, the two-port model was undesirable to use as it does not allow for the manipulation of individual components in the system.

2.5.3 Lumped Parameter

An alternative method is to model the transducer as a network of its individual electrical components. This allows for the individual manipulation and if desired, reconfiguration of the component quantities. This type of model is more flexible than a two-port model, and was suitable for use in this work. With this type of model, computer software such as SPICE can be used to solve for individual quantities, or MATLAB® can be used if the transfer function between known and desired quantities is first determined.

3 Aim of Study

The aim of this work is to use a model of the B71 in conjunction with measured impedance data to simulate the behavior of this BC device in terms of its state variables force, acceleration, and power at the mastoid portion of the human skull. Of particular interest is the variability in output due to variability in the load, and the consequences and causes of this behavior.

Questions that will be addressed in this study:

- How does the variability in output dynamics relate to the variability of human mastoid impedances?
- What is the bias error due to calibration with an artificial mastoid?
- What is the size and variability of the output quantities under the skin at the mastoid?

4 Method

4.1 Measurement of B71 Frequency Response

The frequency response function F_{out}/u_{in} was measured for the Radioear B71 device #86-5. An Agilent 35670A signal analyzer was used for signal generation and measurement, and a B&K Artificial Mastoid type 4930 (Serial #2278234) was used as the load. The stimulating signals u_{in} used were a logarithmic sweep of 401 single-frequency sinus signals ranging from $100 - 10k\ Hz$ and an averaged series of white noise measurements with a frequency range from $100 - 12.8k\ Hz$. Both signals had an RMS voltage of $0.5V$. The signal was sent as input to channel 1 as well as to the terminals of the B71. The B71 was placed in the B&K Artificial Mastoid under a pressure of 5.4 N. The output force signal of the B&K AM was sent to channel 2 of the signal analyzer, and the frequency response function

$$\frac{F_{out}}{u_{in}} \tag{4}$$

was displayed in dB as a function of frequency. The data was imported to MATLAB along with the 401-point frequency vector, and a correction for the frequency dependent force sensitivity of the B&K 4930 AM was applied to the data. The measured frequency response is shown in figure 9.

4.2 Modelling of B71

The model of the B71 used in this work is adapted from Håkansson et al., 1986, and reworked (Håkansson, 2010, personal communication). A schematic is shown in figure 5. The electrical and mechanical parts of the transducer are shown as lumped parameters, and the load which in this case is the mastoid is shown as an unknown impedance. On the electrical side, the source is modeled as an ac voltage source and the transducer's coil ohmic resistance, coil inductance, and frequency-dependent resistance of the magnetic core losses are shown as separate components.

The transduction is represented by two dependent voltage sources, which model the interaction between the velocity of the suspended plate and the current throught the coils. A transduction constant g relates the velocity v on the mechanical side to the current i on the electrical side. The compliance and damping of the transducer suspension are represented in series as C_1 and R_1. The total mass of the armature, bobbins, and wire are represented by m_1. The casing itself has some compliance, mass, and damping and these are represented by C_2, m_2, m_3, and R_2 respectively. The mass of the casing is

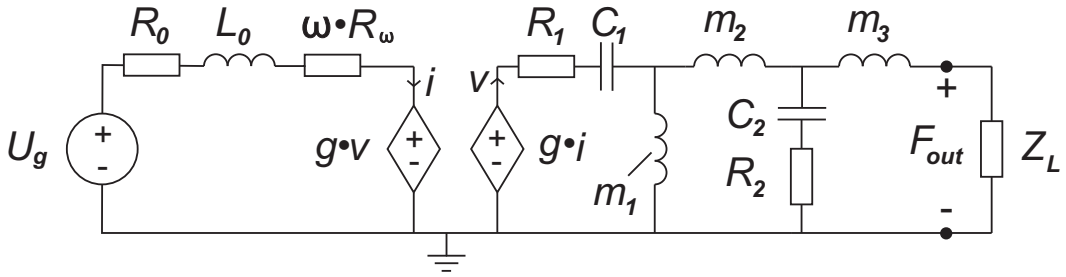

Figure 5: The lumped-parameter model of the B71 with input voltage source U_g and load impedance Z_L

divided among two components as part of the casing is resonant with its own compliance, and the rest is more closely connected to the load. The force and velocity at the interface between the casing and the skin of the subject are represented in the circuit by the voltage and current over the load. By calculating the transfer function in equation 4 in terms of the components, the quantities of force, acceleration, velocity, and power at the load can be estimated. The behavior of this function is best understood by a qualitative description of the circuit, and the calculation of the transfer function can be seen in Appendix A.

Component	Mass(kg)
Bobbin,Coils and Magnet	.01473
Plate	.00217
Casing (Inner half)	.00196
Casing (Outer half)	.00200
Screws (Plate to Magnet)	.00023
Screws (Casing and Vibrator)	.00150

Table 2: Component masses for B71 (Serial #86-5)

4.2.1 Parameter Values

Once the layout of the model is determined, the values of the lumped parameter circuit elements are to be assigned so that the model's performance will closely resemble that of the device being modeled in a simulation.

The lumped parameters that are most easily measured are all the parameters on the electrical side of the circuit - with the exception of the frequency-dependent resistance - and the masses on the mechanical side. The masses of the transducer components as measured on an OHAUS Dial-O-Gram® balance scale are listed in table 2. The values of parameters on the electrical side are taken from the two-port parameter Z_{11} measured for the same

device by Cortes (2002). This parameter is a measure of the impedance of the electrical side of the transducer, and the inductance could be found from the slope of the magnitude, the resistance from the minimum value of the magnitude, and the frequency-dependent resistance from the phase and knowledge of the impedance.

The distribution of the masses to the parameters m_1, m_2, and m_3 as well as the determination of the compliances and damping is determined by a practical understanding of the physical layout of the device along with analysis of the circuit and comparison to actual device performance. Firstly, the mass of the transducer is assigned to m_1. The remaining mass - that of the casing, screws, and the suspended plate is distributed between m_2 and m_3. This distribution as well as the determination of the damping in the system is done by analysis and fitting of the results of simulation to the measured transfer function of the B71, shown in figure 9. As the measured force output in the figure is made with a B&K Artificial Mastoid type 4930 (Serial #2278234) as the load, the load used in the MATLAB simulation is measured impedance data of the same device.

In figure 9 there are three clearly visible peaks at approximately 400, 1450, and 3650 Hz. These peaks correspond to frequencies at which there is electromagnetic or mechanical resonance in the system, and can be used to determine appropriate component values. In an electric circuit, resonance can be seen where there is a combination of inductors and capacitors in series or in parallel, and in cases with sufficiently little damping the resonant frequency can be calculated to be

$$f_r \simeq \frac{1}{2\pi\sqrt{LC}} \tag{5}$$

where L is the value of the inductance in Henry and C is the capacitance in Farads. On the mechanical side, the resonance then depends on the masses and compliances of the system. The B71 has its maximum force output at the 400 Hz resonant frequency, which corresponds to resonance between the transducer mass m_1 with the compliance C_1. The second resonant frequency occurs as an interaction between masses m_2 and m_3 and the compliance and mass of the load, and the 3.7 kHz peak from resonance due to the compliance C_2 of the casing and its mass m_2. Using the measured values for masses and frequencies, the compliances and damping can be estimated. With a numeric approach in MATLAB to find the best fit for the force output curves, the distribution of casing weight between m_2 and m_3 as well as values for the damping constants are found. Figure 9 shows the simulated curve of output force per volt input with the artificial mastoid impedance as load data, along with the measured transfer function F_{out}/u_{in} described in section 4.2. Once the dimensions of the model have been satisfactorily determined, the model can be used to study the output when loaded with different data. This model can thus be used to address the questions presented in section 3.

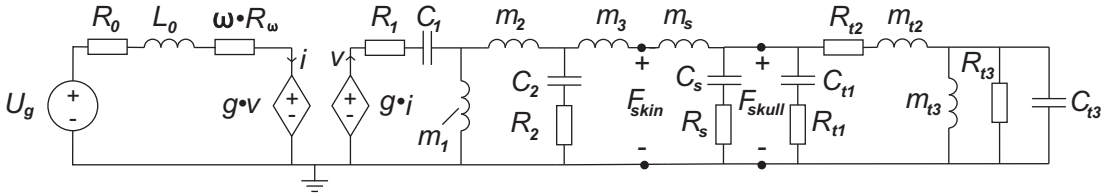

Figure 6: The model of the B71 connected to a model of the skull bone via skin parameters C_s, m_s and R_s

4.2.2 Extension of the Model

To determine the effect of the force, acceleration, and power incident on the skull bone underneath the skin, the impedance of the skull needs to be separated from that of the skin. First a model of the skull impedance through a titanium implant is adapted from Håkansson et al., 1986 by removing the compliance C_0 directly associated with the bayonet coupling between the transducer and the titanium post. An assumed model of the skin with a mass component in series and a compliance and damping component in parallel is connected to this model, and the combination is connected to the model of the B71 (seen in figure 5). The complete model is shown in figure 6. Estimation of the values for the skin mass, compliance and damping is done in two steps:

First, the measured BC impedances seen in figure 7 are assumed to be representable as a three-parameter model as seen in the work of Håkansson et al. (1986). These parameters are estimated for each subject by a division operation in MATLAB corresponding to a least-squares approximation. The median of the estimated three-parameter impedances and the median of the actual mechanical point impedances are compared in figure 14. Next, the input impedance Z_S of the combined model (looking towards the skull from outside the skin, at F_{skin} in figure 6) is calculated while sweeping the parameters C_s and m_s for the skin. Z_S is compared to the three-parameter model for each subject, and the values of C_s and m_s which minimize the rms error between the two are determined for each subject, and stored as the skin compliance and mass. The damping R_s used for each subject is the same as for the three-parameter model of the BC impedance.

4.3 The Simulations

4.3.1 Force Variability

To determine the output force variability's dependence on variability in load impedance, the B71 model was loaded with the measured mechanical point impedance (skin impedance at the mastoid) of 30 different subjects in the frequency range $0.1-10\,kHz$. The data was obtained from Cortes (2002) and

the group consisted of 30 normal hearing subjects - 18 males and 12 females with ages between 22 and 51 and a mean age of 30.6 years (Cortes, 2002, pg. 2). An analysis of the error in these measurements can be found in the work (Cortes, 2002, pg. 5). Figure 7 shows the magnitude and phase of the measured impedances. The complex impedances represented in MATLAB as vectors were used as the load in the model, and the transfer function F_{out}/u_{in} was calculated at each of 801 logarithmically spaced frequencies with a range from $100 - 10000\ Hz$. Please note that a model generator voltage of 1 V was used in all simulations, hence F_{out}/u_{in} may be referred to simply as F_{out} and the transfer function as output force. The acceleration at the skin is determined by differentiation of the velocity through mulitplication with the term $j\omega$

$$a(j\omega) = (j\omega) \cdot v(j\omega) = (j\omega) \cdot \frac{F_{out}(j\omega)}{Z_S(j\omega)} \tag{6}$$

The apparent power output at the skin is also determined using the output force and impedance data by

$$S_{app}(j\omega) = |S(j\omega)| = \frac{|F_{out}^2(j\omega)|}{|Z_S(j\omega)|} \tag{7}$$

4.3.2 Bias Error

To determine the bias error in force threshold measurements due to AM impedance, the force output of the model was calculated using the impedance of the B&K Artificial Mastoid type 4930 (Serial #2278234) as the load. This force is compared at each frequency to the force output from the 30 subjects as calculated in 4.3.1.

4.3.3 At Skull Bone

The estimated parameters C_s, m_s, and R_s for skin compliance, mass and damping were used in the combined model (figure 6), and the transfer function from equation 4 was evaluated for F_{skull}. The parameters for the adapted skull model and for the B71 model were unchanged. From the transfer function, acceleration and power were calculated in the same way as described in 4.3.1.

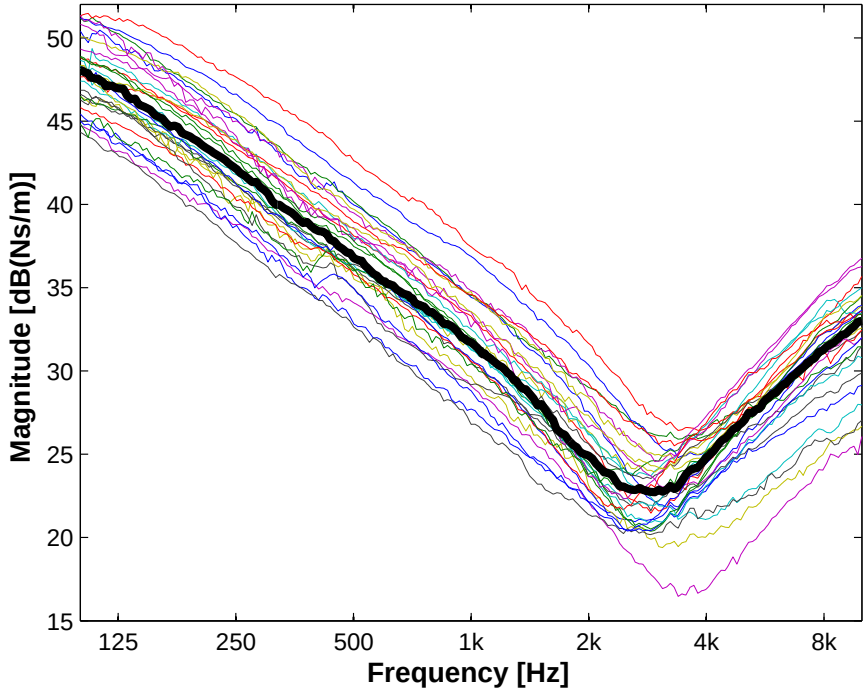

(a)

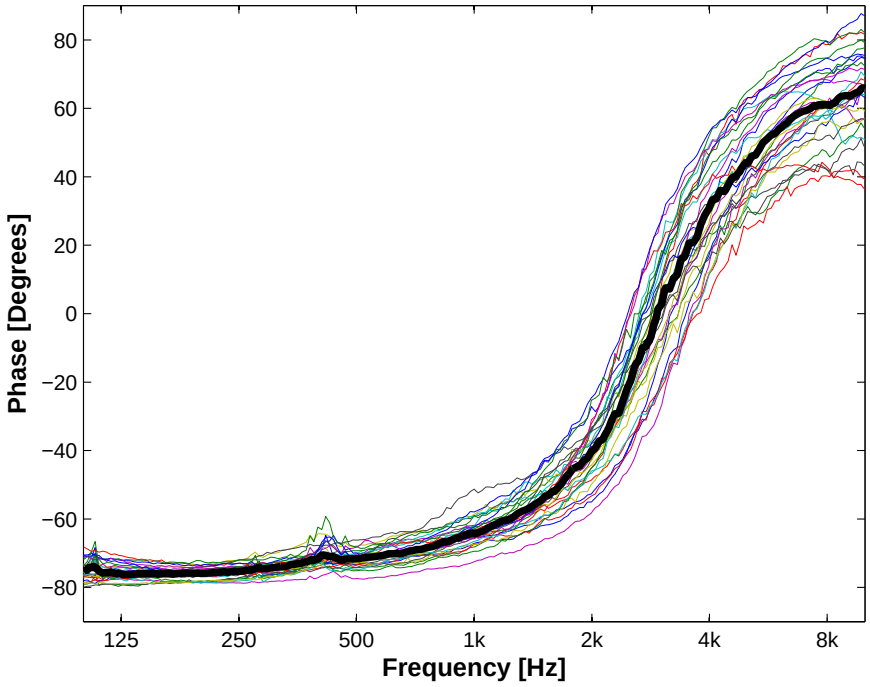

(b)

Figure 7: (a) Magnitude of mastoid mechanical point impedance for 30 subjects, and the median of the magnitudes at each point. Magnitude in dB relative to 1 Ns/m. (b) Phase of the same impedances also including median.

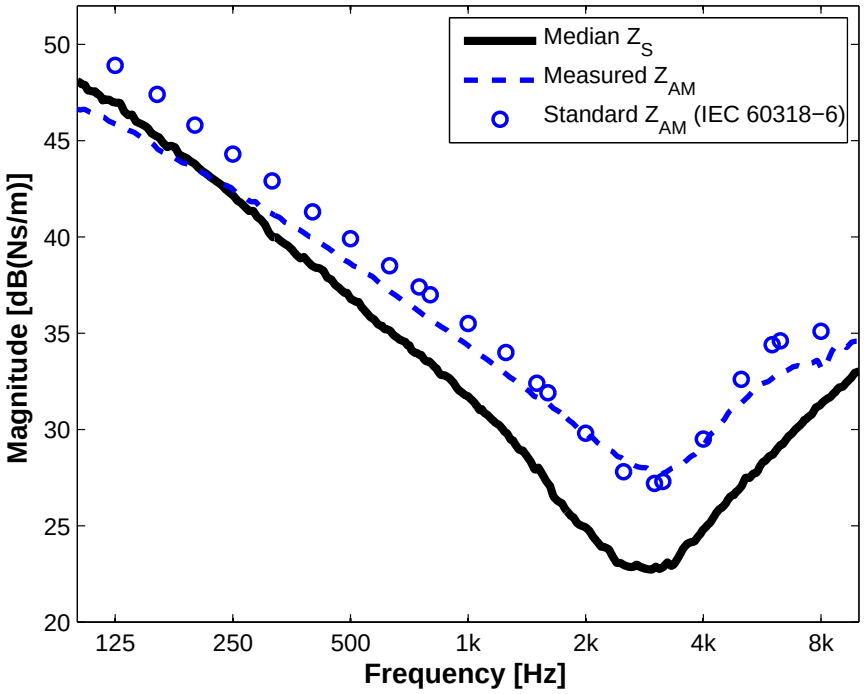

Figure 8: The solid line shows the magnitude of the median measured skin impedance from Cortés (2002). The dashed line is the measured impedance of the B&K Artificial Mastoid type 4930 (Serial #2278234), and the circles show the IEC standards for artificial mastoid impedances.

5 Results

5.1 Measurement of B71 Frequency Response

The measured frequency response of the force output for the B71 #86-5 is plotted in figure 9. Note that the x and y axes are both logarithmic and that the tick markings on the x-axis correspond to the common test frequencies in audiology applications as well as some additional frequencies of interest.

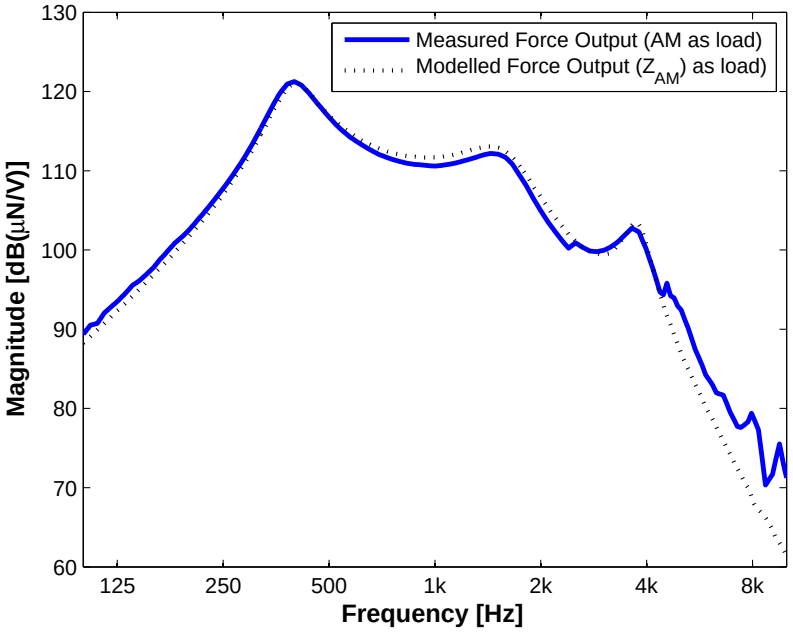

Figure 9: Measured magnitude of the force output of the B71 using AM B&K 4930 as the load, and force output of MATLAB simulation with lumped-parameter model and AM impedance data.

5.2 Output Variability

The transfer function F_{out}/u_{in} for the B71 when loaded with the measured skin impedances (figure 7(a)) is shown in figure 11(a) along with the median force. The corresponding accelerations are shown in figure 12(a), and the apparent power out in figure 13(a).

The variability in impedance, force, acceleration, and apparent power are presented as standard deviations (based on the quadratic differences between the mean values and measured values in dB) in table 3. They are also plotted

in figure 10. Though standard deviation is calculated with reference to the mean, the median was chosen for displaying the results in this work. This is for simplicity as, unlike the mean, the median value is the same for the data and their dB values.

Measure	Min STD [dB]	Max STD [dB]	Mean STD [dB]
Skin Impedance	2.08	2.79	2.44
Force	0.06	4.06	1.71
Acceleration	0.02	4.91	1.60
Power	0.13 (dB Power)	3.66 (dB Power)	1.39 (dB Power)

Table 3: Intersubject variability measured in standard deviation (STD).

5.2.1 Bias Error

The difference in the transducer's mechanical state variables when loaded with the AM and with the mastoid impedances is seen in figures 11(b)-13(b). The difference in force, acceleration and power between the AM and the median subject ranges from zero to more than twice the standard deviation of intersubject variability.

5.3 At Skull Bone

The values for the force at the skull bone for the 30 subjects including the median are shown in figure 15(a). Figure 17(a) shows the magnitude of the force on the skull bone of the 30 subjects and their median is shown together with the median of the force at the skin. The ratio between the median forces are shown in figure 17(b)

The estimated three-parameter model of the skin impedance, and the subsequent three parameters used to model the skin's contribution to the model including the extended skull part were found to be very similar, with the mean compliance differing most (approximately 5%). The averages of the three parameters used to estimate the measured skin impedance were $m_{Sest} = 7.6 * 10^{-4}$, $C_{Sest} = 4.2 * 10^{-6}$, and $R_{Sest} = 14.0$. The mean of the parameters used in the extended model to characterise the skin alone were $m_S = 7.6 * 10^{-4}$ $C_S = 4.0 * 10^{-6}$ and $R_S = 14.0$.

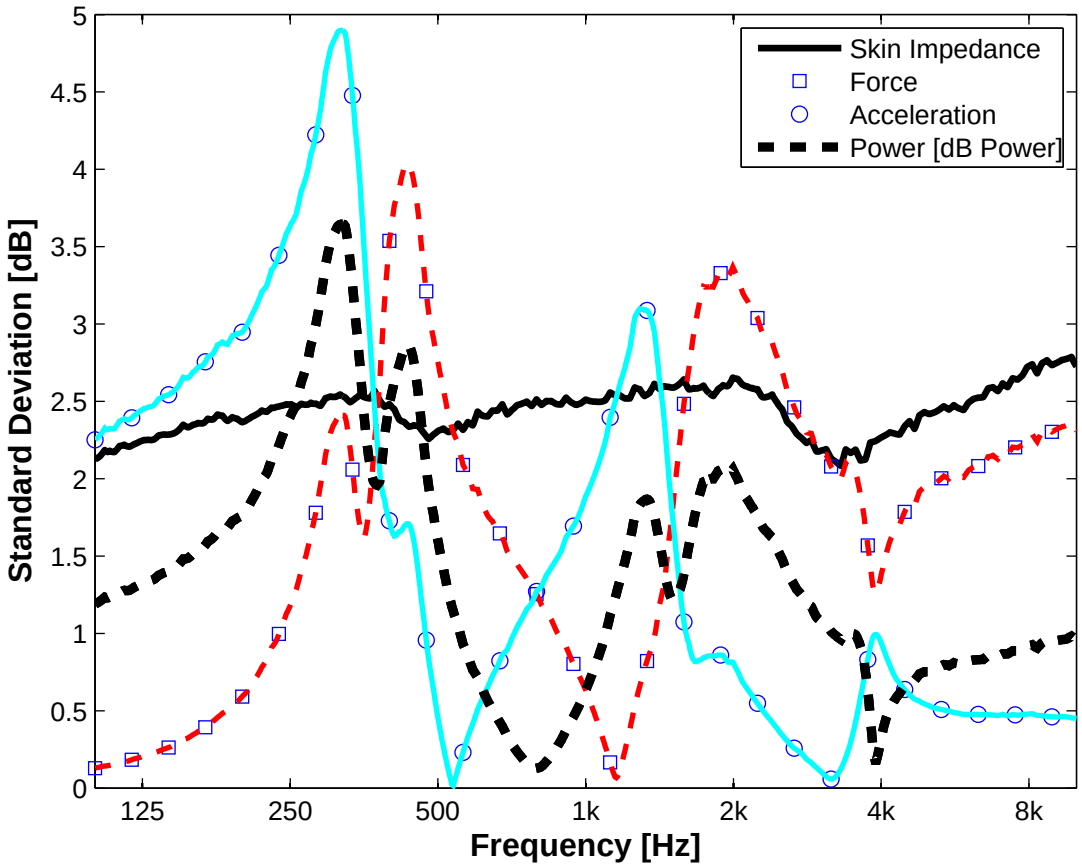

Figure 10: Standard deviation of impedance, force, acceleration, and power at the skin of the 30 subjects.

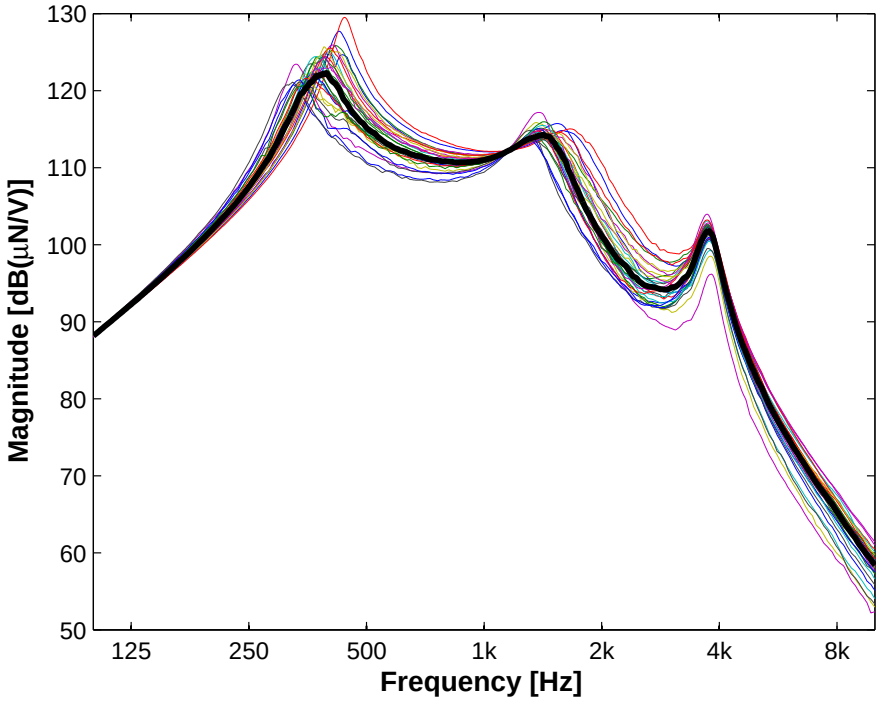

(a)

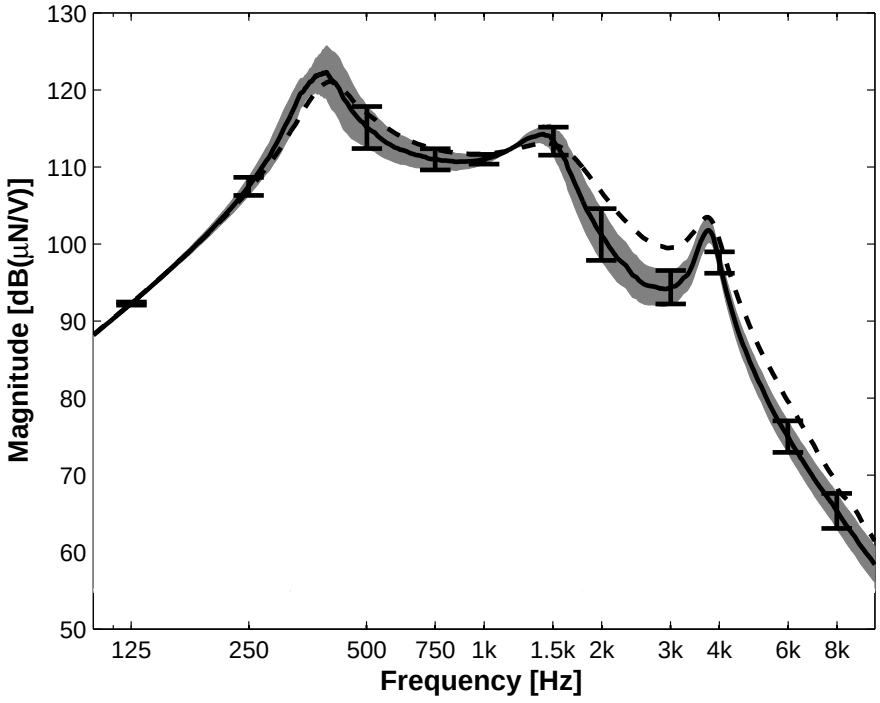

(b)

Figure 11: (a) Magnitude of the output force at the skin of 30 subjects. Force is displayed in dB relative to 1 μN per Volt input. (b) Median output force at the skin of 30 subjects and output force with the artificial mastoid as the load. The shaded area and the error bars show the range of the median force plus/minus the standard deviation.

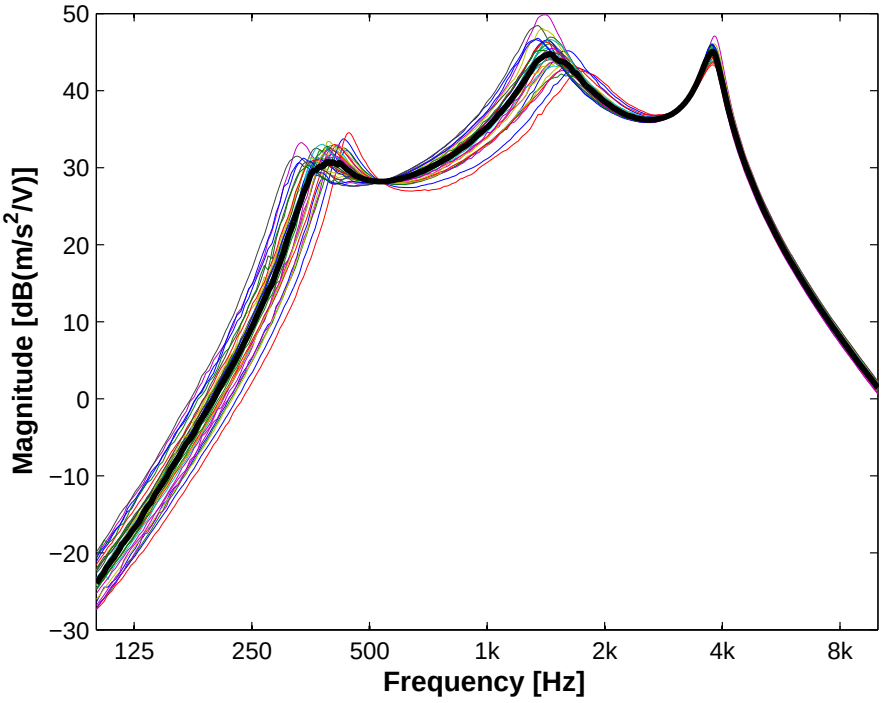

(a)

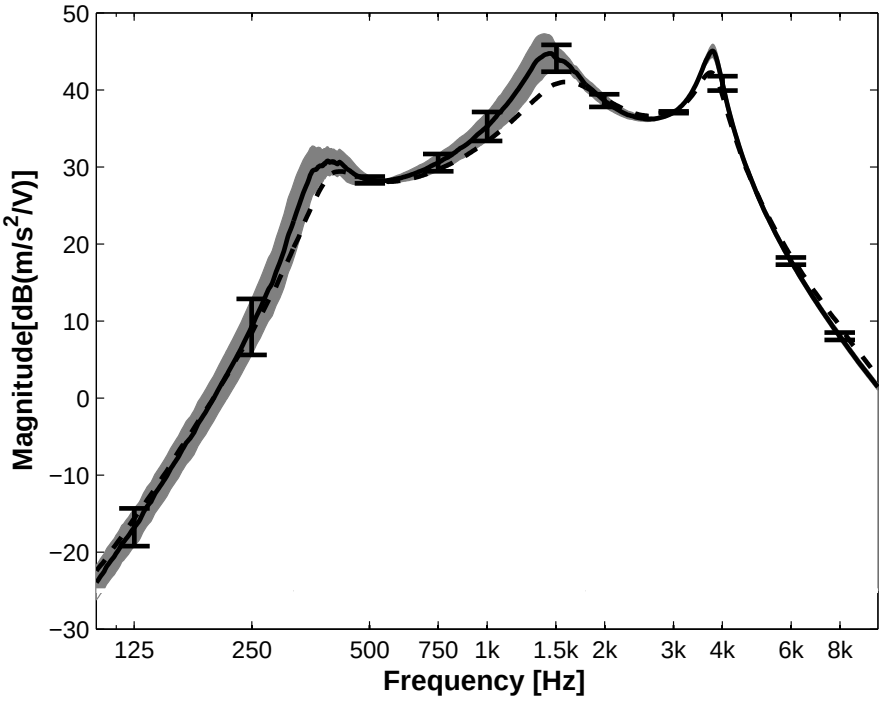

(b)

Figure 12: (a) Magnitude of the output acceleration at the skin of 30 subjects. Acceleration is displayed in dB relative to 1 m/s^2 per Volt input. (b) Median magnitude of output acceleration at the skin of 30 subjects and output acceleration with the artificial mastoid as the load. The shaded area and the error bars show the range of the median acceleration plus/minus the standard deviation.

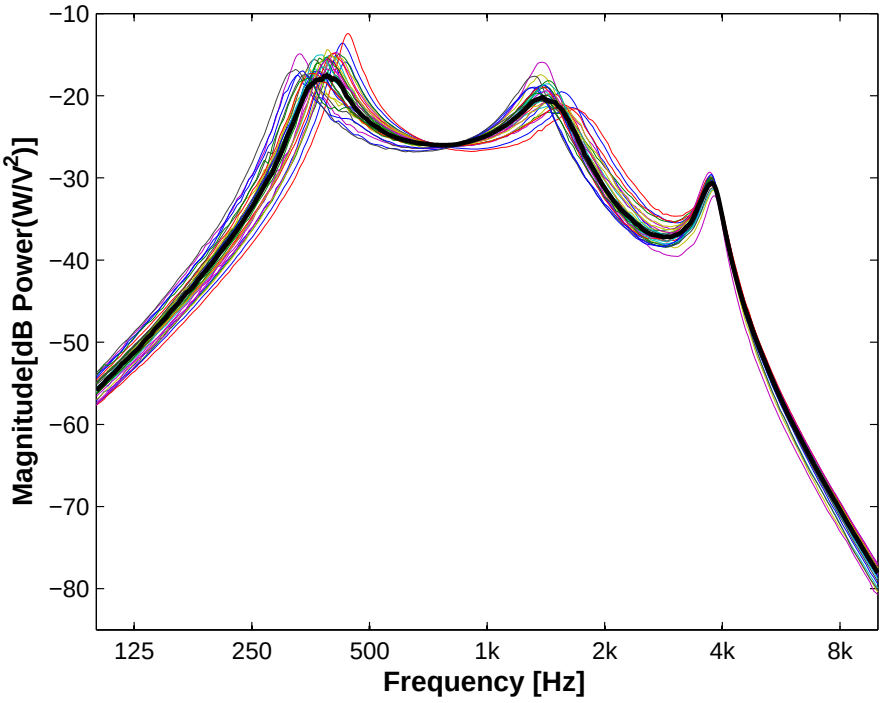

(a)

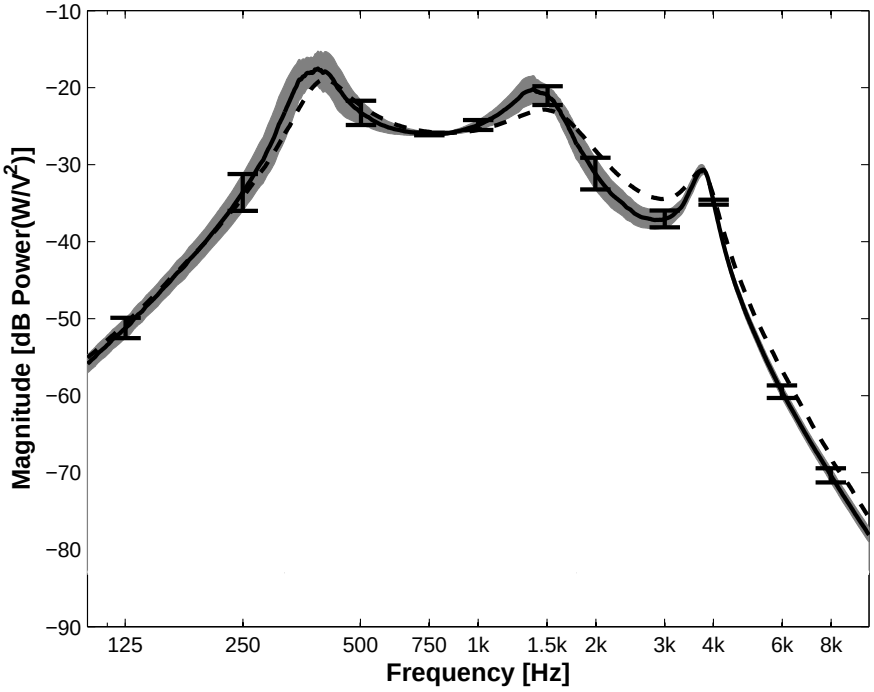

(b)

Figure 13: (a) Magnitude of the apparent power output at the skin of 30 subjects. Power is displayed in dB power relative to 1 W per Volt^2 input. (b) Median apparent power at the skin of 30 subjects and with the artificial mastoid as the load. The shaded area and the error bars show the range of the median power plus/minus the standard deviation σ.

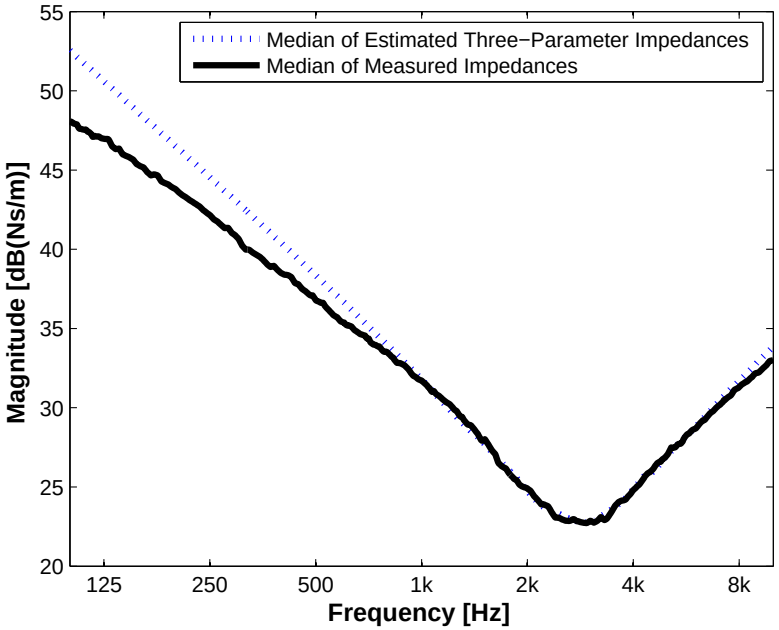

Figure 14: The magnitudes of the median impedances from the three-parameter estimated model and measured skin impedances from Cortes, 2002.

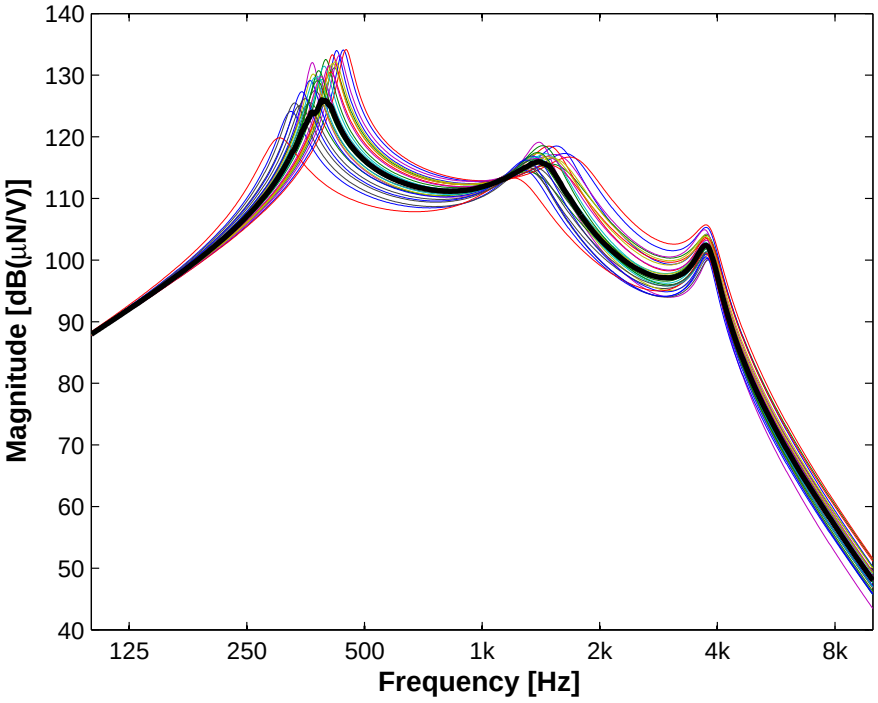

(a)

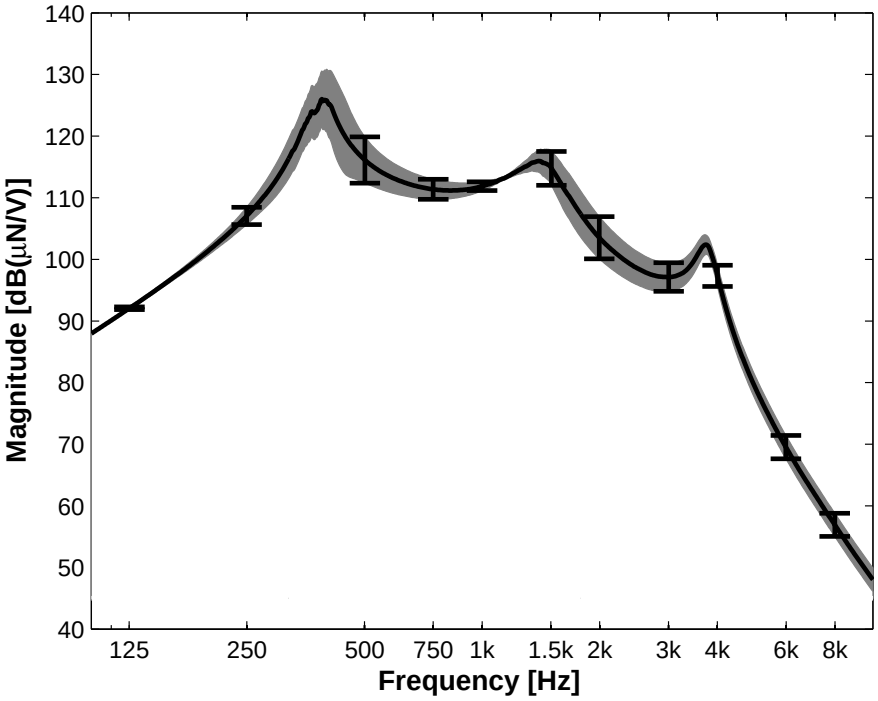

(b)

Figure 15: (a) The dB magnitude of the force on the bone at the mastoid of 30 subjects and their median. (b) Median force at the bone and region encompassing plus/minus one standard deviation.

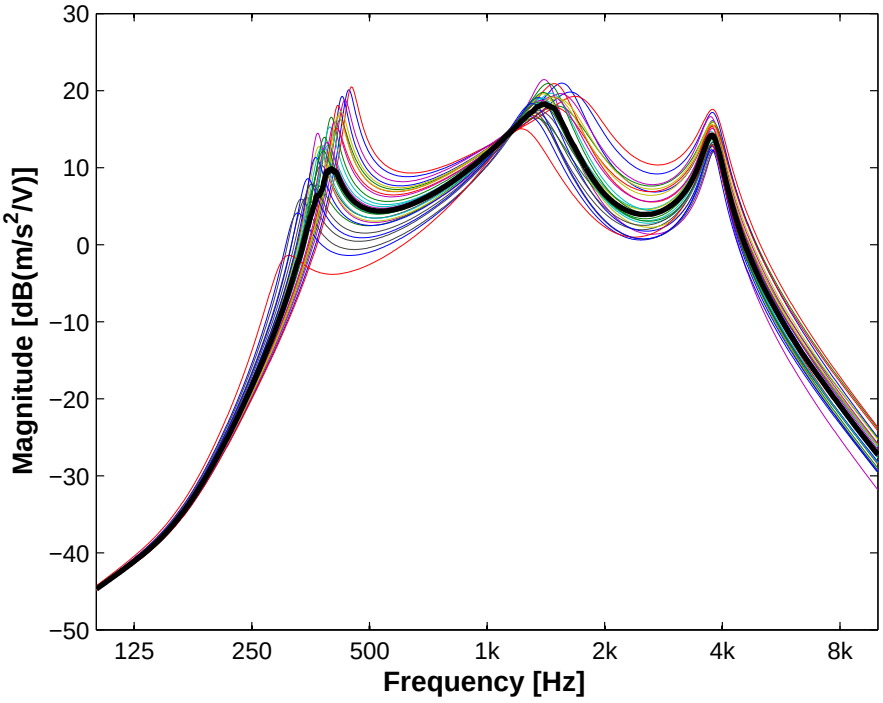

(a)

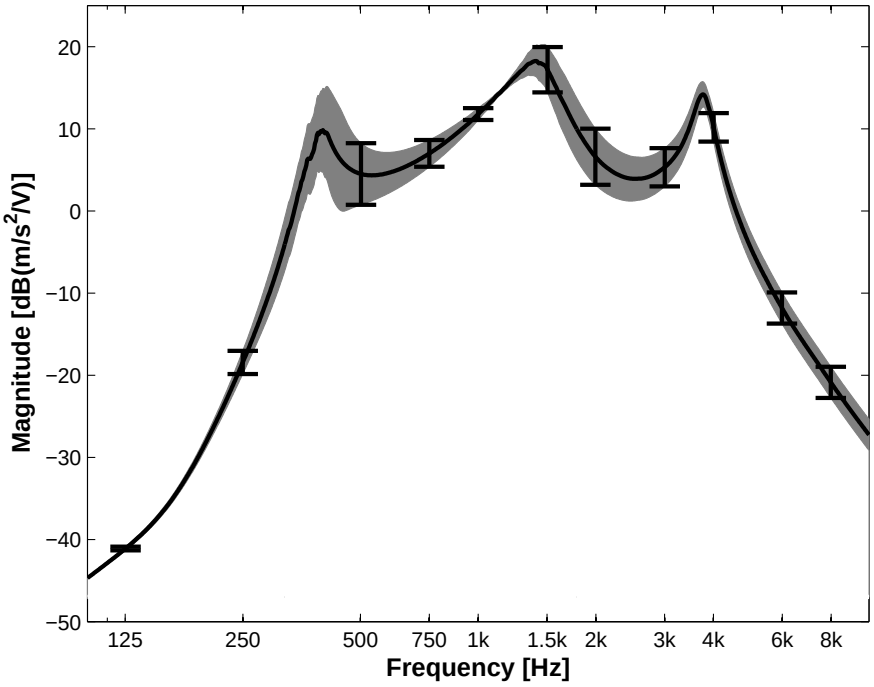

(b)

Figure 16: (a) The dB magnitude of the acceleration on the bone at the mastoid of 30 subjects and their median. (b) Median acceleration at the bone and region encompassing plus/minus one standard deviation.

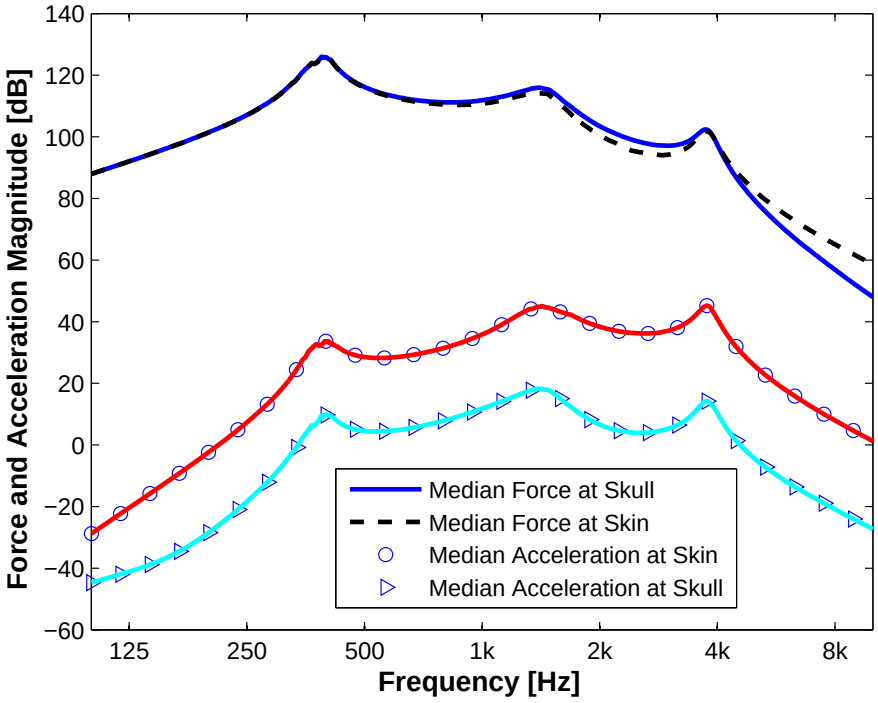

(a)

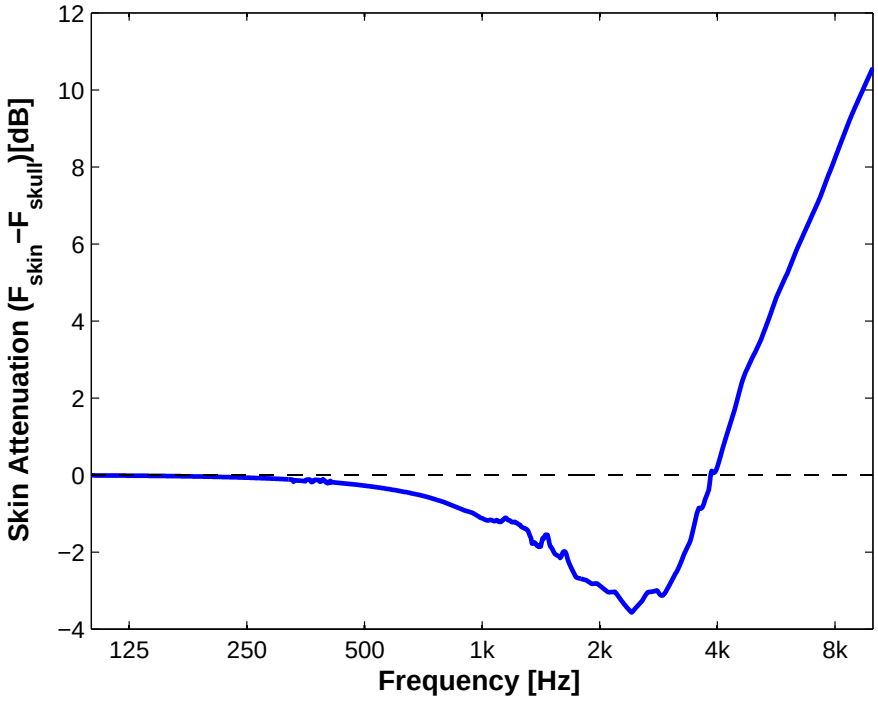

(b)

Figure 17: (a) The dB magnitude of the force and acceleration outputs at the skin and at the skull bone per volt input for the B71 # 86-5. (b) The dB force difference across the skin F_{skin}[dB]-F_{skull}[dB]

6 Analysis and Discussion

6.1 The Models

The lumped-parameter models used to simulate the transducer and load are fairly accurate, as shown in figure 9. The basis for the accuracy of the transducer model is this comparison to the measured output force per volt and the average force difference over the entire range is less than 2 dB. The average force difference in the frequencies above 4 kHz is in the order of 5 dB. The accuracy of the model in the upper frequencies is therefore lesser than between 0.3 and 4 kHz, where the average error is 0.3 dB, which can be considered negligible. The fitting of the model parameters to the measured output force per volt input of the transducer uses only one set of measured impedances for the AM, and one set of measured force data. As is discussed below, AM impedance varies with a number of conditions including how recently it has been calibrated.

The validity of this model may therefore be greatest when it is used to produce relatively quantifiable data and not absolute quantities. The comparison of variability in load impedance to that of output state variables such as force and acceleration is a useful application for this model, while it may be less suitable for determining absolute quantities such as the peak force produced. The model can also be used to determine the effects of altering parameter values, or introducing new components into the system and comparing the behavior to a control simulation.

The extension of the model to include the model of the skull also has the greatest validity when used to compare different simulation results to one another. The adoption of three parameters to model the skin impedance was done with a minimization of rms difference over the range $1.3 - 7.5$ kHz only. This was done as the mass effects of the whole skull determine the curvature of the skin impedance at the lower frequencies, and this mass could not be included in a three-parameter model. Consequently, the extended model may have a lesser validity under 1 kHz. As the B71 has limited performance at the low end of it's frequency range, the accuracy of the model may not be critical in the low frequencies.

6.2 The Simulations

6.2.1 Variability

The variability (expressed in terms of standard deviation or STD) of the force, acceleration, and power varies substantially over the simulated range compared to the load impedance. For example, table 3 shows that the standard deviation of the acceleration has a maximum of 4.91 dB, which corresponds to a range with a maximum value of nearly 20 dB, and a minimum value of 0.02 dB. The STD's of the force and power vary similarly, in con-

trast to that of the load impedances, which is quite constant over the entire frequency range. The standard deviation above and below the median is represented by the shaded region in figures 11(b)-15(b), but may be interpreted more accurately by the size of the error bars in regions with large slope.

The resonance frequency of the skin impedances as well as the the lower two resonant frequencies of force, acceleration, and power at the skin have significant variability as well. The highest resonance frequency in the output force, acceleration, and power is relatively constant for all subjects. The qualitative description of the contributors to each resonance given in section 4.2.1 are simplifications, as can be seen from the difference between the measured resonant frequencies and those obtained using the lumped parameter values and equation 5. The impedance of the load apparently contributes substantially to the first resonance frequency as well as the second one as was mentioned above. The constancy of the third (highest) resonant frequency indicates independence of the variability in load impedances, and is consistently found at ≈ 3.75 kHz for the output force, acceleration, and power.

As the successful calibration of an audiometer to absolute zero gives a reference that is based on an average of a group of normal-hearing individuals, it may be assumed that the error due to intersubject variability is negligible. When force thresholds are determined for an individual, however, the uncertainty is as large as the variability in force seen in figure 11(a). Under the assumption that other sources of error such as those listed in section 2.3.2 are ignored, this alone can still account for up to 10 dB error at some frequencies.

Another source of error that should be mentioned here is the variability of AM impedances. These devices were originally designed to have a frequency-dependent impedance conforming to standard normal impedance, and should be calibrated to this standard. This calibration is not entirely simple, however, and the impedance of the artificial mastoid is sensitive to age, quality and temperature of the rubber parts. The error due to variability in AM impedance results in a difference in audiometric zero, and should be considered together with that of intersubject impedance variability.

From figures 11(a), 11(b), 12(a) and 12(b), it can be seen that the points where the STD's of the force, acceleration and power become very small are quite well defined, meaning that at these frequencies, the particular output quantity (force, acceleration or power) is independent of the load's variability (within the range of loads studied). In the force plot, this point lies at 1148 Hz and in the acceleration plot at 537 and 3162 Hz. From figure 10 it can be seen that the STD of the power (measured in dB Power) behaves as the product of the force and acceleration variabilities - having all the same maximums, but having minimums where force and acceleration STD curves cross each other. The frequencies where power has minimal variability are 790 and 3.9k Hz.

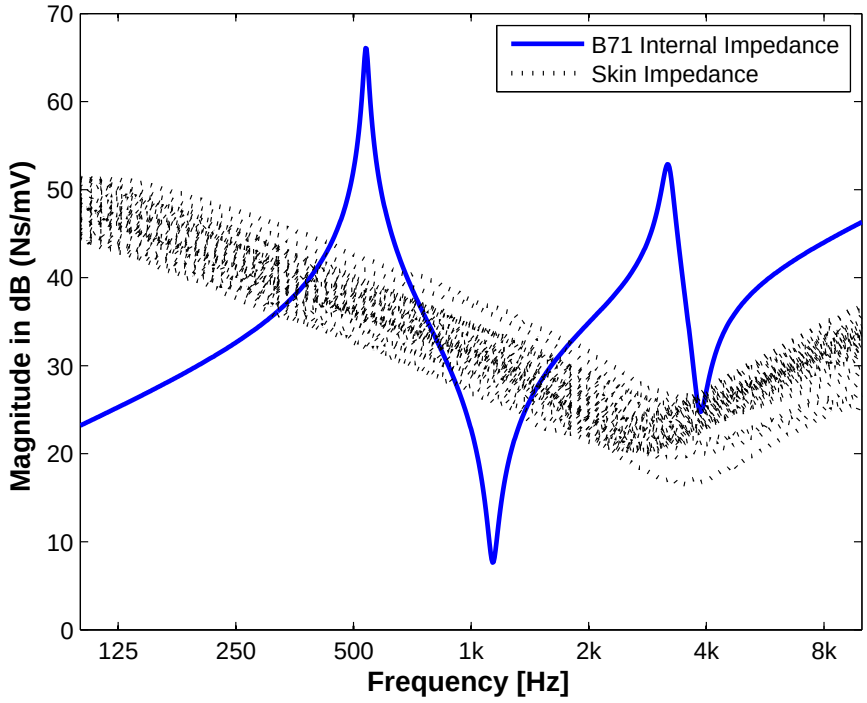

Figure 18: The internal (output) impedance Z_{out} of the B71 together with the skin impedances Z_S of the 30 subjects. Magnitude is expressed in dB relative to 1 Ns/m per Volt input.

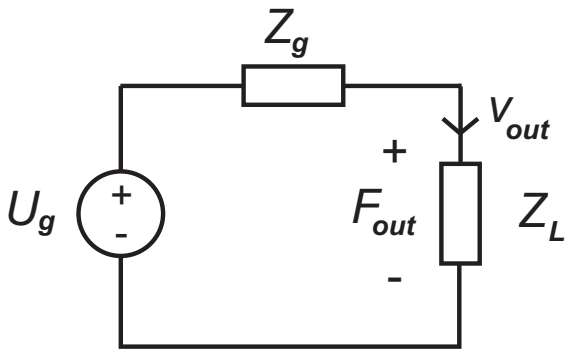

Figure 19: A representation of the system as a Thévenin equivalent of the B71 and the load Z_L

This behavior is best understood by considering the system's Thévenin equivalent as in figure 19, and the relation between the internal impedance

of the B71 (found by measuring the impedance at the output port with the voltage source short-circuited) and the skin impedance as in figure 18. When the load impedance (in this case the skin impedance Z_S)is much greater than the internal output impedance of the transducer, the B71's behavior will approach that of an ideal voltage generator - i.e. the impedance of the load will determine the voltage (force) across it regardless of the internal impedance. When the internal impedance is much greater than the load impedance ($Z_g \gg Z_L$) , the B71 will approach an ideal current generator in it's behavior, providing a constant current (velocity) at the load. In figure 18, the points where the internal impedance Z_g has sharp peaks due to series and parallel resonances, it differs maximally (between 25 and 30 dB) from the median skin impedance. These resonant peaks correspond with the points of minimal standard deviation in figures 11(a) and 12(a). The second series resonance at approximately 4 kHz does not coincide with such a point, as Z_g and Z_L are of approximately the same magnitude at this point.

These points of negligible variability in force and acceleration are of potential value in the calibration stage of audiometery, particularly the 1148 Hz frequency in the force. If the internal impedance of a BC transducer in the lab is known, the calibration of the transducer/audiometer with an artificial mastoid to audiometric zero will be most reliable at this frequency. The sensitivity of the measured force to variations from standard in AM impedance will be minimized, providing the most accurate measure of the transducer's output condition. This point would also be the most reliable at which to take threshold measurements. From figure 11, it is apparent that the STD is small only at a very well-defined point, and the closest audiometry test frequency 1000 Hz has a greater intersubject variability in the force, though smaller than the average.

It is of interest to consider acceleration - having two such points of independence of load impedance - as the reference for audiometry. Both the mean and standard test frequencies standard deviations of intersubject variability are lesser for the acceleration than for the force (though not substantially), an argument for the use of RETAL's (Reference Equivalent Threshold Acceleration Levels) instead of RETFL's. These quantities are both valid measures of the level of stimulation from the transducer, but some arguments can be made for the choice of force over acceleration. It is pointed out by Håkansson et al. (1985) that the acceleration is relatively sensitive to the condition of the skin and the contact area, due to it's dependence on the values of C_s and R_s (see figure 6). This depence is confirmed by observing figure 17(a), which shows that the acceleration level is substantially lower under the skin than at the skin, whereas the force is less dependent on skin condition.

The power is also interesting to consider as a reference. It is poorly understransferedtood which factors contribute most to hearing, and one could argue that since the power is most closely related to the total energy transfered to the skull, it could also be the best measure of what finally leads to

stimulation of the hair cells in the cochlea. The power is represented here as the apparent power - the vector product of the real power which is dissipated as friction, and the reactive power which results in elastic movement and averages zero. Whether the best measure of transferred energy is reactive, apparent, or real power is a discussion that may not be done justice here, as it requires a better understanding of the mechanical transfer dynamics from the surface of the skull to the cochlea.

The "golden" frequencies, where the state variables reach their minima in variability vary depending on what quantity is of interest, but hold interest with regards to interpretation of results that depend on these outputs as the most reliable frequencies to observer when load impedance is unknown and hence causes uncertainty. The region $500-1200$ Hz has a high concentration of these frequencies, as can be seen in figure 10.+

6.2.2 Bias Error

The difference between the output state variables due to the difference in impedance between Z_{AM} and Z_S is considerable at some frequencies and zero at others, as mentioned in section 5.2.1. Here we will discuss what relevance and meaning this difference has. As there are many uncertainties regarding threshold determination, the least of which being whether or not output force is a valid measure of hearing, a few assumptions and simplifications are first proposed:

- We will assume that force on the skin is a valid measure of hearing. This is fundamental in audiometry as the measure of hearing levels is closely related to output force levels.
- We will assume that the average otologically normal and normal hearing person is the average of a large number of subjects and that their skin impedances Z_S average out to the mean or median Z_S shown in this work (mean and median are very similar in this case).
- We will also assume that the mean or median skin impedance Z_SM gives rise to the mean or median output force in figures 11(a) - 13(b) when used as the load. This has been verified in MATLAB as a reasonable assumption.
- Finally, we will assume that every artificial mastoid has the same Z_{AM} and every B71 BC tranducer performs identically.

The averaged reference equivalent force RETFL is measured on an artificial mastoid with mechanical point impedance Z_{AM}. Referring to figure 20, we can see that the signal required to produce this force (U_0) is the one that produces the threshold force F_{0M} on the averaged normal-hearing subject

(Subject M) who has median mechanical skin impedance Z_{SM}. The difference between F_{0M} and RETFL is the bias difference seen in figures 11(b) - 13(b) between the dashed black lines and the solid black median line.

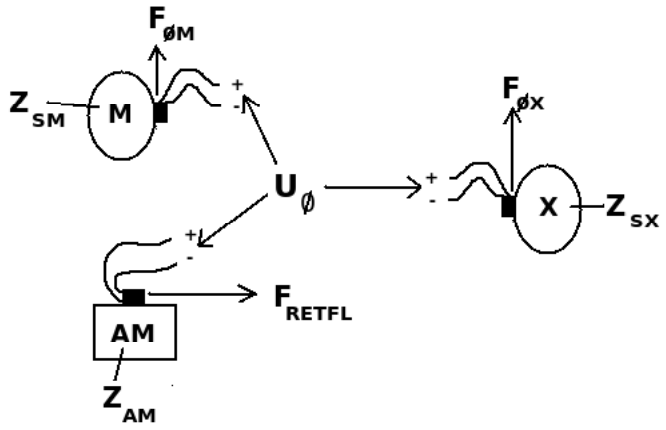

Figure 20: Force outputs from equivalent signal input with different load impedances.

When an audiometric test is done on a subject (subject X in figure 20), the force produced on that subject by input signal U_0 may differ from the force F_{0M} produced on the averaged subject due to a difference in skin impedance. If the subject's skin impedance Z_{SX} is maximally different from median skin impedance Z_{SM}, the forces F_{0X} and F_{0M} produced by input signal U_0 will differ maximally, the magnitude of which can exceed 10 dB at some frequencies, as can be seen in figure 11(a). When the hearing threshold for subject X is found, the dBHL will be shown in dB as

$$20 * log_{10}(U_0/U_{TX}) \tag{8}$$

where U_{TX} is the signal strength at threshold for subject X. Since the dBHL is based on the relation between input signal strengths where the reference U_0 is taken from subject M, the impedance and force on the AM are not factors in the measure of dBHL. In fact, if the last assumption from above held at all times, there would be no need to calibrate the BC transducer using an artificial mastoid. The bias between the median and AM output forces in figure 11(b) is only a measure of the difference between the RETFL and the output force F_{0M}.

The error in dBHL due to this method of threshold determination is limited to the (up to and including) more than 10 dB mentioned due to the difference in force output audiometric zero when signal U_0 is used on

two subjects of differing Z_S. If the last assumption above does not hold, which is likely the case in many testing facilities, there is greater uncertainty, due to the fact that RETFL produced on two AM's of differing mechanical impedances will require different input signal strengths. Data on the actual impedances of a number of AM's is required to quantify this uncertainty.

6.2.3 At Skull Bone

For the extended model, only one set of parameter values was used to represent the impedance characteristic of the skull bone, and everything to the right of the skin parameters C_s and R_s can be looked at as one impedance Z_B (shown as Z_{skull} in figure 21). Since Z_B has such a large magnitude, it would be expected that the force would not differ greatly between the skin and the skull. In figures 17(a) and especially17(b), it is confirmed that the force after transmission through the skin is similar to the force at the skin. It is also apparent that the acceleration is substantially attenuated by the skin, which makes sense when considering the magnitude of C_s and R_s compared to that of Z_B. The skin compliance and damping act as a shunt in the circuit, shunting the velocity (and hence acceleration) to "ground". These results are in good agreement with the work of Håkansson et al. (1985), where the impact of the skin on energy transfer to the skull is discussed. The skin impedance parameters are also similar to their findings. In figure 17(b), it is seen that the force on the skull is at some frequencies actually higher than that of the skin, particularily in the 3 kHz region, where it is amplified by the skin resonance. The mass of the skin m_s becomes dominant in the higher frequencies, attenuating the force.

Looking at figure 16(a), one finds that the points of constant acceleration present at 537 and 3162 Hz are no longer present, and in fact there is only one frequency where the variability in acceleration among the subjects becomes very small, and it is located at approximately 1150 Hz. Figure 22 shows that the skull impedance is substantially larger than the output impedance of the transducer with the skin attached for the entire frequency range. It seems that this would indicate a constant force output, yet the force has a substantial mean intersubject standard deviation. In fact, the force variability is only at a minimum at the same point as it was at the skin, which coincides with the acceleration.

Figure 23 shows the standard deviation among the subjects for the acceleration at the skull bone is very similar to that of the force at the skin, and seemingly identical to that of the force at the skull. This effect can be explained if one again considers the Thévenin equivalent of the transducer including the skin. The mechanical output impedance would be the Thévenin impedance Z_{Th} which varies with the skin impedance, and the Thévenin voltage source is equal to the voltage measured at the load when it is removed, making an open circuit. As the load (the skull bone) has such

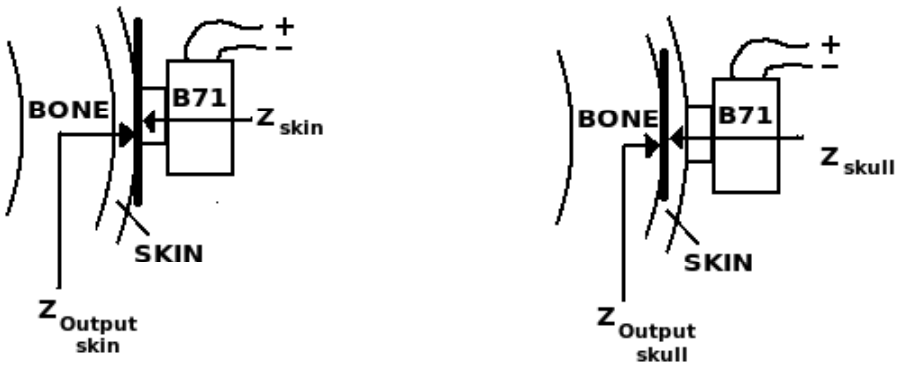

Figure 21: The internal impedance and load impedance seen from the skin/transducer interface and the skin/skull interface.

a large impedance, the voltage across the skin (the skin force from figure 11(a)) can be used. Both of these have only one point of near-zero inter-subject deviation, 1150 Hz, and consequently the variability of the current (velocity) and the force will have a minimum at this frequency, be equal to each other, and dependent on the Thévenin factors when an identical load (the skull bone) is used for each subject. In a model that considered variations in the skull impedances of the 30 subjects, this effect may not be as apparent. In fact, due to this simplification, the observed results under the skin should not be considered as reliable as those showing the behavior of the transducer mechanical state variables at the skin surface.

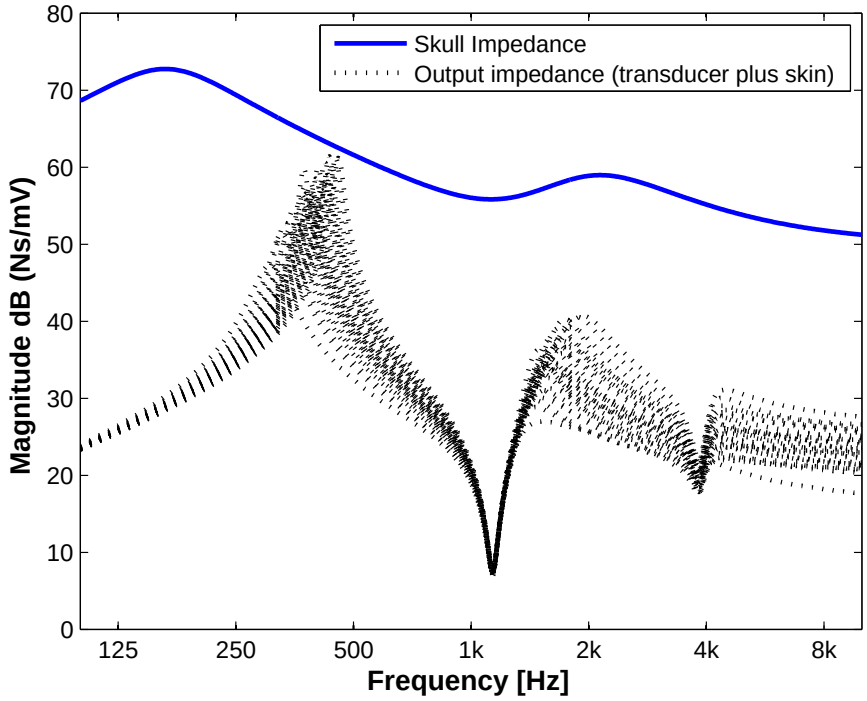

Figure 22: The internal (output) impedance of the B71 and connected skin together with the estimated skull impedance. Magnitude is expressed in dB relative to 1 Ns/m per Volt input.

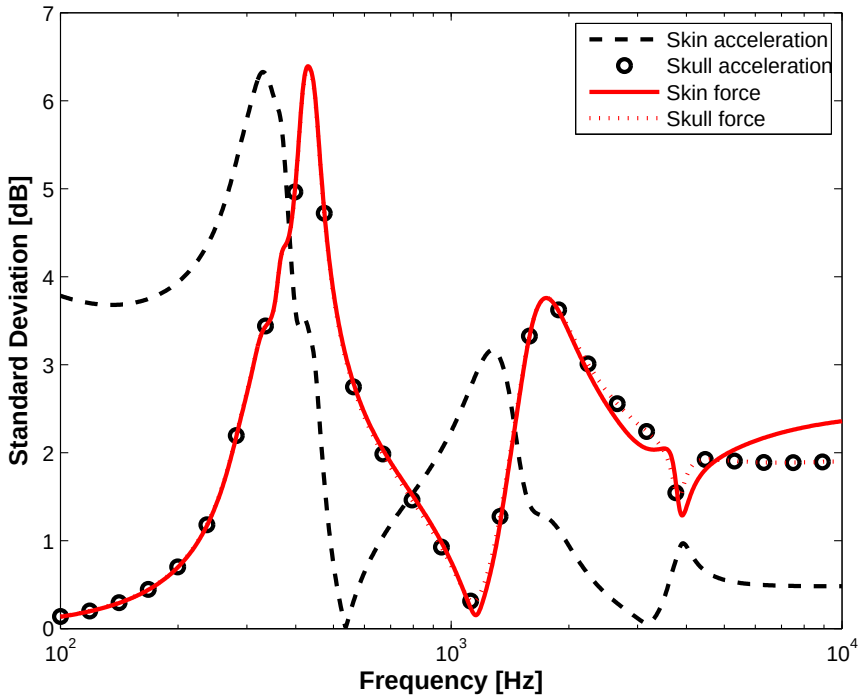

Figure 23: The standard deviation of the force and acceleration at the skin and at the skull bone.

7 Conclusions

With the apparent benefits of percutaneous bone conduction in terms of power consumption, comfort and sound quality, the use of transcutaneous bone conduction transducers is today largely confined to audiology applications. The similarity in magnitude of transducer and load impedances when using a BC driver such as the Radioear B71 makes the sensitivity of the output state variables to variations in load impedance greater than with a load such as the skin-penetrated skull, which has a relatively high impedance.

Much of the motivation for this work lies in the uncertainty associated with BC threshold determination. Quantitative and qualitative knowledge about the extent of variability in transducer output is important for the analysis and reduction of uncertainty when determining BC hearing thresholds. An investigation was done into the behavior of output force, acceleration and power from a lumped-parameter tranducer model when measured skin impedances were used as the load (Measured impedances of 30 normal-hearing subjects were taken from Cortes (2002)). These variables were modelled at the skin surface and also at the skull bone under the skin with a Radioear B71 transcutaneous BC driver.

7.1 Main Points

Some important conclusions of this work include:

- The variability in measured skin impedances used as the load is relatively consistent at all studied frequencies, with an intersubject standard deviation ranging from 2.08 to 2.79 dB.
- The variability in force, acceleration and apparent power at the skin surface fluctuates substantially across the frequency range (100 - 10000 Hz). All three state variable range from less than 0.15 dB STD up to more than 3.5 dB STD, with the acceleration having a maximum of 4.91 dB standard deviation.
- The points at which the variability becomes negligibly small are very well-defined, and their frequencies can be predicted with knowledge of the mechanical output impedance of the transducer and approximate magnitude of skin impedances. These points may be of value in audiology, e.g. for purposes of calibration for audiometry.
- At the skin surface, the points of negligible variability differ for force and acceleration, with one well defined frequency for the force, and two for the acceleration. Under the skin at the skull bone, there is only one such frequency, common to the force and the acceleration.

- The bias between the output state variables when the load is an artificial mastoid and when the load is the *median* human mastoid is predictable and ranges from 0-3 dB Power in the power, 0-5 dB in the acceleration, and 0-6 dB in the force.

- The importance of the artificial mastoid impedance exactly matching that of human mastoid is questionable in with regards to uncertainty in hearing threshold determination. The impedance differences between artificial mastoids and between the subject being tested and the average is of greater relevance.

7.2 Continuation

Doing the simulations has yielded some expected and some unexpected results, and of course has brought up questions that demand further exploration. Further work could be done investigating:

- Clinical or research uses for which the points of constant output acceleration and force can be used.

- The behaviour of the state variables at the skull bone using actual subcutaneous skull impedances. The results at the skull bone obtained in this thesis are based on the assumption of nonvarying subcutaneous skull impedances. Lacking measured skull impedance data, multiparametric sweeps of model variables may give a more accurate portrayal of the subcutaneous dynamics.

- The effect of manipulation of model parameters on any other part of the model can be simulated with relative ease.

- An analysis of all sources of uncertainty or error in the audiometry process, including that due to impedance variabilities. An objective measure of the importance of each source or error could be determined via a mathematical model

8 Acknowledgments

My thanks and gratitude go out to my supervisor Bo Håkanson, for his patience and consideration while explaining many of these concepts to me, for the time he has spent in meetings with me and for his positive attitude and enthusiasm when discussing this work. Also many thanks go to my friend Per Östli, who repeated times spent hours helping me with understanding and implementing different parts of this project, and whose encouragement has made it so much easier to keep going. Finally, thanks to my girlfriend Sara, for her constant and unconditional support and kindness which have helped me to keep my head up and complete these last five years of my education.

A Calculation of Transfer Function

The seven unknown variables i, v, v_{1-4} and F_{out} are represented in as many equations, utilizing Ohm's law, Kirchoff's Voltage law and Kirchoff's Current law. The laplace variable s is used in the derivation for simplicity, but is replaced in MATLAB by $j\omega$.

$$KVL: \quad U_g = i \cdot (Z_1) + g \cdot v \qquad [Z_1 = R_g + R_0 + sL_0 + \omega R_\omega] \quad (9)$$

$$KVL: \quad g \cdot i = v \cdot Z_2 + v_1 \cdot (sm_1) \qquad \left[Z_2 = \frac{1}{sC_1} + R_1\right] \quad (10)$$

$$KVL: \quad v_1 \cdot sm_1 = v_2 \cdot sm_2 + v_3 \cdot (Z_3) \qquad \left[Z_3 = \frac{1}{sC_2} + R_2\right] \quad (11)$$

$$KVL: \quad v_3 \cdot Z_3 = v_4 \cdot (sm_3 + Z_L) \quad (12)$$

$$KCL: \quad v = v_1 + v_2 \quad (13)$$

$$KCL: \quad v_2 = v_3 + v_4 \quad (14)$$

$$Ohm: \quad F_{out} = v_4 \cdot Z_L \quad (15)$$

Combing (13) and (14) gives:

$$v = v_1 + v_3 + v_4 \quad (16)$$

(9) and (10) and (16) give:

$$g \cdot \frac{U_g - g(v_1 + v_3 + v_4)}{Z_1} = (v_1 + v_3 + v_4) \cdot Z_2 + v_1 \cdot sm_1 \quad (17)$$

Rearranging (17) and substitution with Z_4 gives:

$$v_1 = \frac{\frac{gU_g}{Z_1} - v_3 Z_4 - v_4 Z_4}{Z_4 + sm_1} \qquad \left[Z_4 = \frac{g^2}{Z_1} + Z_2\right] \quad (18)$$

Using (14) and (18) in (11) and substitution with Z_5, then rearranging gives:

$$v_3 \cdot \left(\frac{Z_4 \cdot sm_1}{Z_5} + sm_2 + Z_3\right) = \frac{gU_g \cdot sm_1}{Z_1 \cdot Z_5} - v_4 \cdot \left(\frac{Z_4 \cdot sm_1}{Z_5} + sm_2\right) \quad (19)$$

$$[Z_5 = Z_4 + sm_1]$$

Substitution with Z_6 and rearranging:

$$v_3 = \frac{gU_g \cdot sm_1}{Z_1 \cdot Z_5(Z_6 + Z_3)} - v_4 \cdot \frac{Z_6}{Z_6 + Z_3} \qquad \left[Z_6 = \frac{Z_4 \cdot sm_1}{Z_5} + sm_2\right] \quad (20)$$

Using (20) in (12) yeilds:

$$v_4 = \frac{gU_g \cdot sm_1 Z_3}{Z1 \cdot Z_5(Z_6 + Z_3)\left(\frac{Z_6 \cdot Z_3}{Z_6 + Z_3} + sm_3 + Z_L\right)} \quad \left[Z_7 = \frac{Z1 \cdot Z_5(Z_6 + Z_3)}{g \cdot sm_1}\right] \tag{21}$$

Substitution with Z_7 and using (15), then dividing both sides by U_g gives the transfer function:

$$\frac{F_{out}}{U_g} = \frac{Z_3 \cdot Z_L}{Z_7 \cdot \left[\frac{Z_6 \cdot Z_3}{Z_6 + Z_3} + sm_3 + Z_L\right]} \tag{22}$$

B Model Parameter Values

The lumped parameter values used in the models seen in figures 5 and 6 are given here. Units are not shown.

Component	Value
U_g	1
R_0	3.4
L_0	.86e-3
R_ω	$L_0/tan(64.6/180 * pi)$
g	3.3
m_1	16.33e-3
C_1	4.055e-6
R_1	1
m_2	2.56e-3
C_2	1.3e-6
R_2	2
m_3	3.5e-3

Table 4: Values of lumped parameter elements used in model seen in figure 5.

Component	Value
C_S (mean estimated)	$4.2e-6$
m_S(mean estimated)	$7.6e-4$
R_S(mean estimated)	14.0
C_{t3}	$220e-9$
R_{t3}	3800
M_{t3}	2.8
R_{t2}	650
M_{t2}	.09
C_{t1}	$100e-9$
R_{t1}	320
C_{t0} (not used)	$110e-9$

Table 5: Values of median estimated skin parameters, also lumped parameter elements used in model seen in figure 6. All values with the subscript t in their notation are taken from Håkansson et al. (1986).

References

BSA (2002). "Recommended Procedure Pure tone air and bone conduction threshold audiometry with and without masking and determination of uncomfortable loudness levels. *Retrieved April 21, 2010 from http://www.thebsa.org.uk/docs/RecPro/PTA.pdf*".

Cortes, D. (2002). "Bone Conduction Transducers: output force dependency on load condition". Technical report, Department of Signals and Systems, Chalmers University of Technology. SE-412 96 Göteborg, Sweden.

Håkansson, B., Carlsson, P., and Tjellström, A. (1986). "The mechanical point impedance of the human head, with and without skin penetration". *J. Acoust. Am.*, 80(4):1065–1075.

Håkansson, B., Reinfeldt, S., Eeg-Olofsson, M., Östli, P., Taghavi, H., Adler, J., Gabrielsson, J., Stenfelt, S., and Granström, G. (2010). "A novel bone conduction implant (BCI): Engineering aspects and pre-clinical studies". *International Journal of Audiology*, 49(3):203–215.

Håkansson, B., Tjellström, A., and Rosenhall, U. (1985). "Acceleration Levels at Hearing Threshold with Direct Bone Conduction Versus Conventional Bone Conduction". *Acta Otolaryngol*, 100:240–252.

HRF (2009). "John Wayne Bor Inte Här Hörselskadades Riksförbunds Hörselvårdsrapport 2009 *Retrieved March 3, 2010 from http://www.hrf.se/upload/pdf/rapport09.pdf*".

ISO (1994). ISO 389-3 "Acoustics - Reference zero for the calibration of audiometric equipment. Part 3 - Reference equivalent threshold force levels for pure tones and bone vibrators" International Organization for Standardisation. Geneva, Switzerland.

Stenfelt, S. and Håkansson, B. (2002). "Air versus bone conduction: an equal loudness investigation". *Hearing Research*, 167(1-2):1–12.